ACS Catalysis

Review

Cite This: ACS Catal. 2019, 9, 10727−10750

pubs.acs.org/acscatalysis

Overview of Selective Oxidation of Ethylene to Ethylene Oxide by Ag Catalysts

Tiancheng Pu,[†] Huijie Tian,[‡] Michael E. Ford,[†] Srinivas Rangarajan,*[,‡] and Israel E. Wachs*[,†]

[†]Department of Chemical and Biomolecular Engineering and [‡]Operando Molecular Spectroscopy & Catalysis Laboratory, Lehigh University, Bethlehem, Pennsylvania 18015, United States

ABSTRACT: Ethylene oxidation by Ag catalysts has been extensively investigated over the past few decades, but many key fundamental issues about this important catalytic system are still unresolved. This overview of the selective oxidation of ethylene to ethylene oxide by Ag catalysts critically examines the experimental and theoretical literature of this complex catalytic system: (i) the surface chemistry of silver catalysts (single crystal, powder/foil, and supported Ag/α-Al_2O_3), (ii) the role of promoters, (iii) the reaction kinetics, (iv) the reaction mechanism, (v) density functional theory (DFT), and (vi) microkinetic modeling. Only in the past few years have the modern catalysis research tools of in situ/operando spectroscopy and DFT calculations been applied to begin establishing fundamental structure−activity/selectivity relationships. This overview of the ethylene oxidation reaction by Ag catalysts covers what is known and what issues still need to be determined to advance the rational design of this important catalytic system.

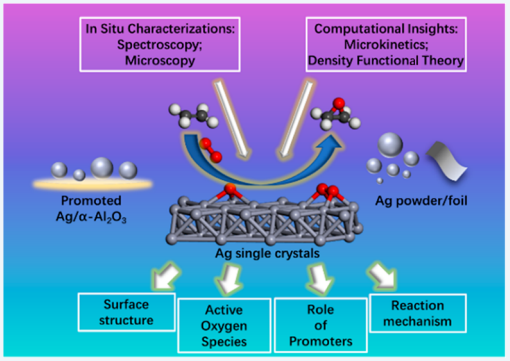

KEYWORDS: *ethylene epoxidation, silver, promoters, catalyst characterization, DFT, kinetics, mechanism, microkinetic modeling*

1. INTRODUCTION

U.S. natural gas production has increased dramatically owing to technological advances in horizontal drilling and hydraulic fracturing.[1,2] The ethane present in natural gas is primarily being tapped to produce ethylene, which is one of the primary building blocks of the petrochemical industry.[3] As a consequence, the ethylene production in the U.S. was estimated to increase by at least 8 megatons by the end of 2017.[4,5] Ethylene oxide (EO) is one of the major chemicals produced annually from ethylene, with the United States being the largest producer.[6] Ethylene oxide is an important chemical intermediate that is further converted to major consumer products such as antifreeze, pharmaceuticals, detergents, and plastics. In 2016, the worldwide production of EO was 34.5 million tons with a compound annual growth rate of 4.3% between 2011 and 2016. This growth rate is estimated to annually continue at ∼2% for 2017−2021.[7]

Industrially, EO is currently produced by gas-phase selective ethylene oxidation (ethylene epoxidation) that is typically performed in fixed-bed tubular reactors with supported Ag/Al_2O_3 catalysts at 230−270 °C and 1−3 MPa.[8] The EO selectivity is the most important parameter that determines the performance of an EO catalyst. The desired selective epoxidation of ethylene to ethylene oxide is accompanied by two highly thermodynamically favored side reactions: total combustion of ethylene (ΔH of −1327 kJ/mol) and combustion of ethylene oxide (ΔH of −1223 kJ/mol). These side reactions present great challenges for reaching high selectivity to ethylene oxide. Selective ethylene oxidation and the unselective side reactions are indicated by the following set of reaction equations:

$$C_2H_4 + (1/2)O_2 \rightarrow C_2H_4O \quad \Delta H = -105\ \text{kJ/mol} \tag{1}$$

$$C_2H_4 + 3O_2 \rightarrow 2CO_2 + 2H_2O \quad \Delta H = -1327\ \text{kJ/mol} \tag{2}$$

$$C_2H_4O + (5/2)O_2 \rightarrow 2CO_2 + 2H_2O \quad \Delta H = -1223\ \text{kJ/mol} \tag{3}$$

There currently are two types of industrial catalysts employed for EO manufacture: supported Re/Cs/Ag/Al_2O_3 catalysts that operate in excess C_2H_4/O_2[9] and alkaline-metal (Na,[10] Cs[11])-promoted supported Ag/Al_2O_3 catalysts that operate in excess O_2/C_2H_4.[6] Oxides of Mo[9,12] and S[12,13] have been found to also promote the supported Re/Cs/Ag/Al_2O_3 system for EO formation. In addition, $C_2H_4Cl_2$ is also added to deposit Cl on the catalyst, which acts as a promoter. The EO selectivity for an unpromoted silver catalyst approaches 50%,[14,15] while a good industrial promoted catalyst can achieve an EO selectivity in excess of 90%.[16]

Ethylene epoxidation by silver catalysts continues to be a very active research topic because of its practical importance and unresolved fundamental questions surrounding this catalytic system.[17,18] The chronology of publications devoted to catalytic ethylene oxidation since 1980 is presented in

Received: August 14, 2019
Revised: October 9, 2019
Published: October 18, 2019

DOI: 10.1021/acscatal.9b03443
ACS Catal. 2019, 9, 10727−10750

Figure 1 and shows the explosion of publications over the past three decades. Publications prior to 1980 mainly focused on

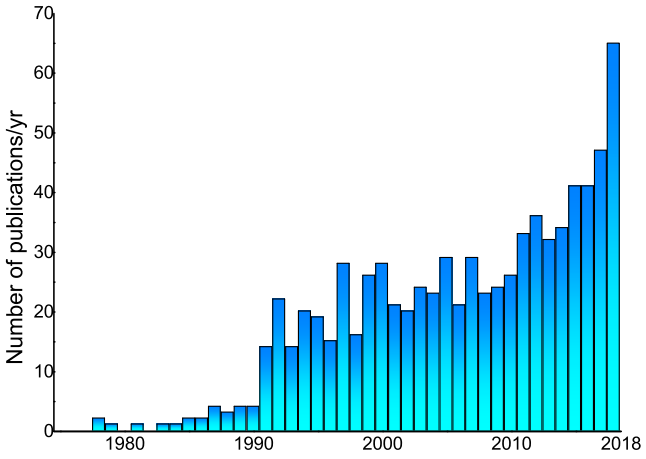

Figure 1. Chronology of number of annual publications devoted to the topic of ethylene epoxidation (data obtained from Web of Science, key word search "ethylene", "oxidation" and "Ag").

evaluating catalytic performance (conversion and EO selectivity) and reaction kinetics. The publications after 1980 have emphasized catalyst surface structures and reaction intermediates in order to determine the unique characteristics of silver catalysts for high EO selectivity.

Several reviews of ethylene oxidation by silver catalysts have appeared over the years. Van Santen and Kuipers reviewed the literature prior to 1987 with a focus on surface science studies on Ag single crystals and mechanistic studies of ethylene epoxidation over supported Ag catalysts. The review highlighted the uniqueness of Ag as an ethylene epoxidation catalyst due to the (i) Ag−O bond strength, (ii) chemical nature of adsorbed oxygen species, and (iii) inability of Ag−O to activate the C−H bond of ethylene. It also proposed that application of in situ characterization studies of supported Ag/Al_2O_3 catalysts would lead to significant progress in the field.[14] More than a decade later, Serafin, Liu, and Seyedmonir summarized the EO literature prior to 1998. The research findings from temperature-programmed reaction (TPR), Raman spectroscopy, and scanning tunneling microscopy (STM) on Ag single crystals was reviewed.[17] Serafin et al. concluded that alkaline and halide promoters exhibit both electronic and geometric effects on the surface of Ag single crystals for ethylene oxidation. Furthermore, the surface of the Ag crystal undergoes reconstruction on exposure to Cl_2 and O_2.[17] In 2013, Ozbek and van Santen provided a summary and perspective on fundamental insights from theoretical computational methods for understanding the reaction mechanism of ethylene epoxidation by model Ag single-crystal surfaces.[19] Many of the investigations over the past two decades have focused on well-defined Ag single crystals under ultrahigh-vacuum (UHV) conditions. Studies with supported Ag catalysts at higher pressures have received much less attention. The inability of the ethylene oxidation reaction by Ag to proceed under UHV conditions, however, limits the information about ethylene epoxidation by Ag that can be derived from single-crystal studies.

Despite the large volume of published investigations, very few studies have comprehensively integrated density functional theory (DFT) and in situ catalyst characterization studies during ethylene oxidation by silver catalysts to determine the fundamentals of this catalytic system. Consequently, many critical questions about this important catalytic reaction still remain unresolved. (i) Which oxygen species is responsible for the selective oxidation of ethylene? (ii) Which oxygen species is responsible for the combustion of ethylene and ethylene oxide? (iii) What are the surface reaction intermediates during ethylene oxidation by Ag catalysts? (iv) What are the reaction mechanisms for ethylene epoxidation and combustion? (v) How does each promoter interact with the alumina-supported Ag catalysts and influence conversion and selectivity? (vi) Why are Ag catalysts unique for selective ethylene epoxidation in comparison to other transition metals (e.g., Au and Cu)?

In this context, the literature on ethylene oxidation is reviewed here to provide a systematic and critical analysis of active site and mechanism of this chemistry on different Ag catalysts. We begin with a discussion of studies involving various surfaces of Ag (section 2): viz., Ordered Silver Single Crystal Catalysts (section 2.1), Silver Powder/Foil Catalysts (section 2.2), and Supported Ag Catalysts (section 2.3). We then discuss the kinetics (section 3) and mechanism (section 4) of this oxidation reaction. Finally, investigations employing ab initio calculations (section 5) and microkinetic modeling (section 6) are also covered. Throughout, the complementarity of experiments and computations in unraveling this important catalytic reaction system will be highlighted. Furthermore, the current thinking and ongoing debates will be summarized and suggestions will be made, as needed, on potential experiments and computations that can address the critical gaps in the fundamental understanding of this catalytic system.

2. SURFACE CHEMISTRY OF SINGLE CRYSTALS, POWDERS/FOILS, AND SUPPORTED SILVER CATALYSTS

2.1. Ordered Silver Single-Crystal Catalysts. *2.1.1. Protocols Employed in Studying Ethylene Epoxidation by Ordered Silver Single-Crystal Catalysts.* Ordered silver single crystals under UHV conditions provide well-defined catalytic surfaces that allow for detailed analysis of the interactions between the reactants (ethylene and oxygen) and products (ethylene oxide, CO_2, and H_2O) with the silver surface. The cleanliness of silver single crystals is assured by sputtering and annealing pretreatments and confirmed with Auger electron spectroscopy (AES)[20,21] and X-ray photoelectron spectroscopy (XPS) surface analysis.[22,23] Information about the structural arrangement of the surface Ag atoms and the distribution of reactants on the Ag surface can be obtained from low-energy electron diffraction (LEED)[20,24] and scanning transmission microscopy (STM),[25,26] respectively. The vibrational methods of infrared reflection absorption spectroscopy (IRAS),[27,28] surface-enhanced Raman spectroscopy (SERS),[65] and electron energy loss spectroscopy (EELS)[29,30] provide fundamental details about the molecular nature of oxygen species and surface intermediates interacting with the Ag surface. Electronic information about the oxygen species and the Ag sites in the surface region can be accessed with X-ray photoelectron spectroscopy (XPS).[22,23] Recent XPS technological advances are now also allowing near-ambient-pressure X-ray photoelectron spectroscopy (NAP-XPS) measurements under the reaction conditions.[31] The surface chemistry of the reactants and products with the Ag surface is typically probed with temperature-programmed reaction (TPR)[30,32,33] spec-

DOI: 10.1021/acscatal.9b03443
ACS Catal. 2019, 9, 10727−10750

troscopy, which provides information about reaction pathways and their kinetics.[32,34]

2.1.2. Surface Chemistry of Ordered Silver Single-Crystal Catalysts. Many fundamental studies with model Ag single crystals have been reported.[20,21,32,33,35−39] Early surface science studies of the interactions between different Ag crystal planes with O_2, CO ,and CO_2 were reported by Campbell and co-workers.[38] It was observed that the Ag(110) surface forms adsorbed oxygen adatoms (O_a) upon dosing with gaseous molecular O_2 at 477 K. Subsequent dosing with CO_2 at 380 K leads to formation of surface carbonates ($CO_2 + O_a \rightleftharpoons CO_{3a}$). Isotope-labeling studies revealed that, upon heating, the surface CO_{3a} decomposes by exchanging oxygen atoms between the adsorbed CO_2 and surface O_a.[37−40] This isotope exchange process suggests a protocol for measuring the number of active surface O_a sites of Ag catalysts under oxidizing conditions with $C^{18}O_2$.[41] The surface O_a sites could also be quantitatively reacted on the Ag(110) surface at 310 K by gaseous CO to produce CO_2 ($CO + O_a \rightarrow CO_2$). The peak temperatures for CO_2 formation during CO-TPR were observed at 310 and 550 K and assigned to the removal of surface O_a and near surface O_a, respectively.[38]

Barteau et al. investigated ethylene adsorption on Ag(110) with precoverage of oxygen atoms (O_a) under UHV conditions but did not find any reaction between ethylene and the preoxidized Ag surface.[42] Campbell et al. also found no reaction between ethylene and preadsorbed oxygen on Ag(110) under UHV conditions.[33] In contrast, Grant et al. reported that dosing ~5×10^6 L of O_2 at 300 K onto a clean Ag(111) surface results in atomic O_a located within the surface ($\theta < 0.1$) and chemisorbed dioxygen (O_{2a}) ($\theta < 0.015$) from angle resolved (AR)-XPS and AES surface analysis.[21] During O_2-TPD, O_2 was evolved at 380 and 580 K and assigned to desorption of O_{2a} and O_a from the Ag(111) surface, respectively. No supporting data, however, were provided to confirm the nature of the two adsorbed oxygen species. Ethylene was found to slowly chemisorb onto the oxidized Ag(111) surface at 300 K and selectively react with the surface O_a species to form ethylene oxide, as shown in Figure 2, since the same EO evolution TPR spectrum was observed in the absence and presence of the low-temperature oxygen species (the proposed surface O_{2a} species).[32] Isomerization of ethylene oxide to acetaldehyde over the oxidized Ag(111) surface was also examined, and the rate-determining step (rds) was found to depend on temperature: EO isomerization was the rds below 410 K, and EO adsorption was the rds above 410 K.[43] The above studies reveal that the ethylene oxidation reaction does not take place on Ag single-crystal surfaces under UHV conditions and much higher pressures are required to activate the oxidized silver surface for ethylene oxidation.

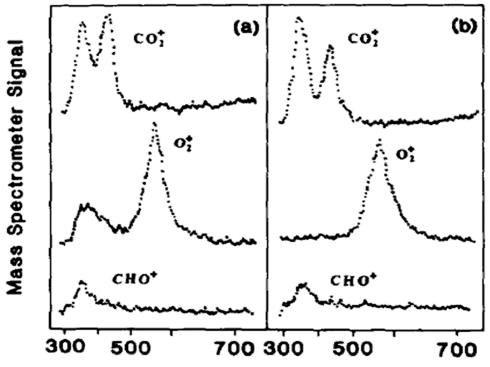

Figure 2. TPR spectra for C_2H_4 oxidation on oxidized Ag(111): (a) Iin the presence of dioxygen; (b) without dioxygen. The O_2 dose was 5×10^6 L followed by a C_2H_4 dose of 9×10^6 L. Heating rate: 13 K s^{-1}.[32] The CHO^+ represents the EO cracking product in the mass spectrometer. Reproduced with permission from ref 32. Copyright 1985 Elsevier.

Bao et al. employed in situ SERS to monitor the nature of the oxygen species present on Ag(110) and Ag(111) surfaces at elevated pressures (0.2 bar of O_2) and temperatures (300−900 K).[44] Three Raman bands were observed at 954, 802, and 632 cm^{-1}, with their distribution dependent on oxidation conditions, and were assigned to adsorbed O_a, subsurface atomic O, and atomic O dissolved in the bulk, respectively. The interactions of the oxygen species with ethylene (0.05 bar and 580 K) revealed the preferential interaction of the subsurface atomic O (802 cm^{-1}) with ethylene. No supporting data, however, were provided for the atomic oxygen assignments, since this study predates the period where DFT codes became available. Nevertheless, this study reveals that the oxygen species on Ag associated with the Raman band at 802 cm^{-1} is involved in the ethylene oxidation reaction.

Linic et al. employed high-resolution electron energy loss spectroscopy (HREELS) to investigate ethylene oxide adsorption and reaction on the Ag(111) surface under UHV conditions.[30] Given that adsorbed C_2H_4 and surface atomic oxygen do not react under UHV conditions,[42] the surface reactivity of EO was investigated by invoking the concept of "microscopic reversibility", which states that the reaction path is the same for the corresponding forward and reverse reactions.[45] The adsorption of EO was examined from 110 to 250 K, and the resulting surface intermediate species were monitored with HREELS. A stable surface intermediate was observed at 250 K that DFT calculations suggested to be a surface oxametallacycle, as shown in Figure 3. Further, the

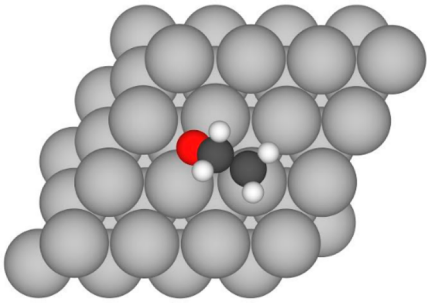

Figure 3. Atomic structure of the proposed surface oxametallacycle intermediate on Ag(111). Color code: Ag, silver; C: dark gray, O, red; H, white).

vibrations observed at 450, 860, 1090, and 2850−2950 cm^{-1} (Figure 4i,c) were assigned to ring deformation via C−C−O stretching, CH_2 rocking, ring deformation via C−C stretching, and C−C and CH_2 stretching of the oxametallacycle, respectively.

Temperature-programmed reaction (TPR) was used to monitor the reaction products from the decomposition of the surface oxametallacycle intermediate. The surface oxametallacycle intermediate reacted at 300 K to yield gaseous EO, CO_2, H_2O, and CH_3CH_2OH desorption products (Figure 4ii). The corresponding DFT calculations proposed that the surface oxametallacycle intermediate is the common precursor for

DOI: 10.1021/acscatal.9b03443
ACS Catal. 2019, 9, 10727−10750

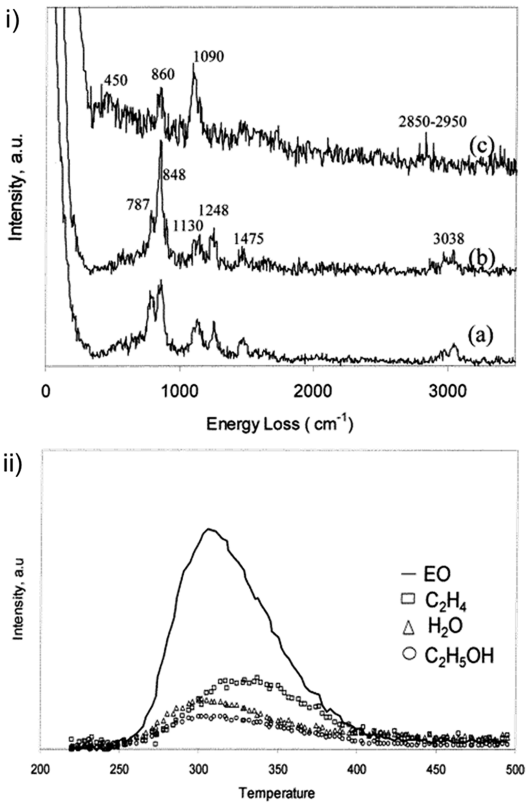

Figure 4. (i) HREEL spectra collected after adsorbing EO to Ag(111) at varying temperatures: (a) 110 K; (b) 140 K; (c) 250 K. (ii) TPR spectra following adsorption of EO on Ag(111) at 250 K.[30] Reproduced with permission from ref 30. Copyright 2002 American Chemical Society.

formation of both the selective ethylene oxide product and unselective acetaldehyde (AA) intermediate that further oxidizes to combustion products.[30] This reaction mechanism has subsequently been widely adopted in the catalysis literature, but it must be kept in mind that the metallic Ag surface in this investigation is likely not the activated silver oxide surface under ethylene oxidation reaction conditions.

Grant, Campbell, and co-workers also examined the addition of Cl and Cs promoters on Ag(110) and Ag(111) surface upon ethylene oxidation (typical conditions: P_{E2} = 4.1 Torr, P_{O2} = 150 Torr, and T = 490 K).[46−50] The promoting elements were introduced by a variety of methods: thermal evaporation source to introduce Cs[46] and dosing with chlorine atoms.[48,50] Temperature-programmed reaction of ethylene on the oxidized Ag crystal surface promoted with Cl was found to inhibit both EO and CO_2 production, but CO_2 production was more strongly inhibited.[48] It is generally accepted that Cl decreases the heat of adsorption of gaseous molecular O_2 through an electronic effect.[51,52] Isomerization of ethylene oxide over Cs-promoted Ag(111) was suppressed by the presence of Cs.[43,51]

2.2. Silver Powder/Foil Catalysts. *2.2.1. Protocols Employed in Studying Ethylene Epoxidation by Silver Powder/Foil Catalysts.* In contrast to ordered and well-defined Ag single crystals, silver powder/foils do not possess ordered surfaces and have much higher surface areas (~1 m^2/g for powder/foils).[53,54] The Ag powders may also contain surface impurities, because it is not possible to clean the surfaces by sputtering and annealing.[55] Such surfaces are typically exposed to oxidation (O_2)−reduction (H_2) treatments that remove surface carbonaceous deposits and some inorganic species. The conducting Ag powders, such as the Ag single crystals, are readily amenable to surface composition analysis by AES,[56] XPS,[53] and low-energy ion scattering (LEIS) spectroscopy.[57] Although STM cannot be performed on the disordered Ag powders, some information about the surface order can be obtained from atomic force microscopy (AFM),[58] transmission electron microscopy (TEM),[26] and scanning electron microscopy (SEM).[9,59] An advantage of these techniques is that recent instrumental advances are now allowing such measurements to be conducted under the reaction conditions. The disordered surfaces of the Ag powders will also not allow EELS surface analyses of adsorbates. The vibrational spectroscopy of IRAS[27,28] and Raman,[60] however, can provide molecular details about the nature of the surface

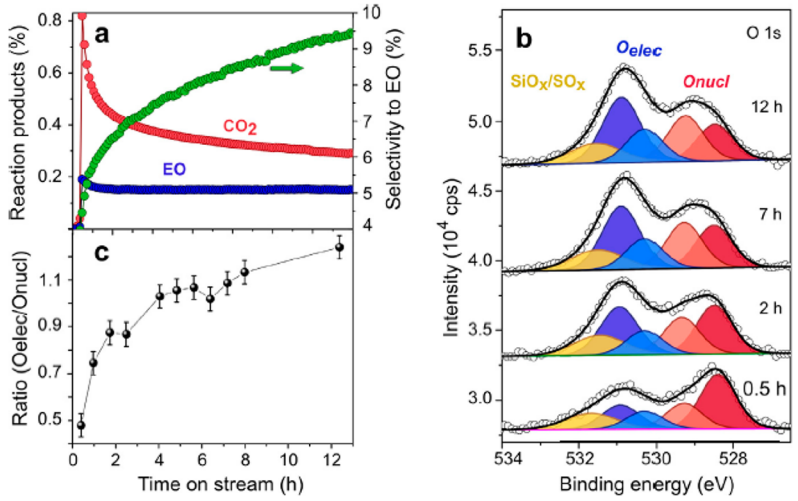

Figure 5. Dynamics of unpromoted silver foil catalyst during ethylene oxidation at 0.3 mbar, 230 °C, and C_2H_4/O_2 = 1/2: (a) mole fraction of reaction products CO_2 (red) and EO (blue) together with selectivity to EO (green) as a function of time; (b) representative O_{1s} XPS spectra measured at different times; (c) ratio of electrophilic to nucleophilic oxygen species (O_{elec}/O_{nucl}) as a function of time.[53] Reproduced with permission from ref 53. Copyright 2014 Elsevier.

DOI: 10.1021/acscatal.9b03443
ACS Catal. 2019, 9, 10727−10750

oxygen species and reaction intermediates. A unique advantage of Raman with Ag surfaces is that it can give rise to surface-enhanced Raman spectroscopy (SERS), which can increase the intensity of the Raman vibrational signal by as much as a factor of 10^6.[61,62] The phenomenon is due to the enhancement in the electric field of the rough Ag surface that increases the intensity of the Raman signal by the incident photons for adsorbates.[63] A particular advantage of Raman on Ag surfaces is that surface roughness enhances the electric field, which in turn increases the intensity of the Raman signal of the surface adsorbates by as much as 10^6. This surface enhancement phenomenon is utilized in the technique of surface-enhanced Raman spectroscopy (SERS), which allows for analyzing surface species on low-surface-area Ag powders (<1 m^2/g). Ultraviolet−visible (UV−vis) diffuse reflectance spectroscopy complements the vibrational spectroscopy methods and provides electronic details about the domain size of Ag clusters and Ag oxidation state, but the signal will be dominated by the bulk contributions because of the low surface areas.[64] An advantage of both Raman and UV−vis spectroscopy is they can be conducted under the reaction conditions. Electronic information about the oxygen species and the Ag sites in the surface region can be accessed with X-ray photoelectron spectroscopy (XPS) under UHV and also NAP-XPS under the reaction conditions.[31] The surface chemistry of the reactants and products with the surface of the Ag powder can be probed with TPR spectroscopy and steady-state reaction studies that provide information about reaction pathways and their kinetics.[32,34]

2.2.2. Surface Chemistry of Silver Powder/Foil Catalysts. Rocha et al. applied operando NAP-XPS and online proton-transfer reaction mass spectrometry (PTRMS) to examine the different oxygen species present and their roles during steady-state ethylene oxidation (C_2H_4/O_2 = 1/2) by Ag foil catalyst at 230 °C and 0.3 mbar, and the findings are presented in Figure 5.[53] The activity of the Ag foil catalyst decreased with time, as reflected in the decreasing production of CO_2. The production of EO remained relatively constant with reaction time, thus, the EO selectivity monotonically increased with reaction time. The simultaneous *operando* NAP-XPS surface analysis revealed that the ratio of the electrophilic oxygen-O_{elec} (core−electron binding energy (BE) of 530.5 eV) to nucleophilic oxygen-O_{nucl} (core−electron BE of 528.2 eV) on the Ag surface significantly increased with reaction time.[22] The relative abundance of these two surface atomic oxygen species on the Ag catalyst during ethylene oxidation, especially the increasing O_{elec}/O_{nucl} ratio, was found to correlate with the increasing selectivity toward EO. This suggests that weakly bonded electrophilic oxygen (O_{elec}) promotes selective EO formation, while strongly bonded nucleophilic oxygen (O_{nucl}) is detrimental to the selective oxidation of ethylene.[22,34] This operando NAP-XPS study, however, did not provide information about the molecular nature of the oxygen species and surface $C_xH_yO_z$ reaction intermediate(s). However, the operando NAP-XPS surface analysis measurements were performed at pressure (0.3 mbar) much lower than those used under conventional EO reaction conditions (>1 bar). Nevertheless, these new fundamental insights are of great significance to understanding this catalytic system.

Bukhtiyarov et al. observed that treating a clean silver foil surface with C_2H_4 and $^{16}O_2$ at 470 K and 0.1 mbar (5% C_2H_4) resulted in the selective formation of electrophilic oxygen, as evidenced by the sole existence of the 530.6 eV peak in the XPS spectrum.[53] Further adsorption of $^{18}O_2$ at 470 K and 1 Pa resulted in formation of surface nucleophilic ^{18}O (BE = 528.4 eV) (Figure 6i). After adsorption of ethylene at 0.1 mbar, the

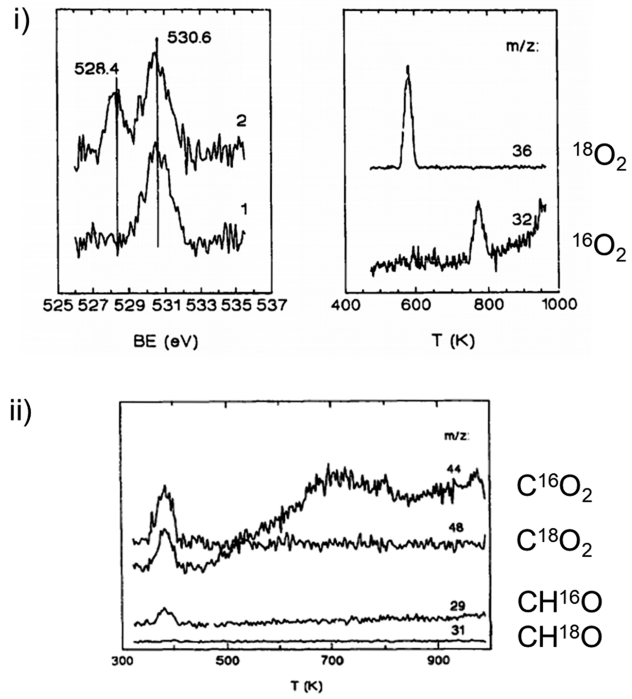

Figure 6. (i) XPS O_{1s} spectra (left) and TPD spectra of O_2 (right) recorded after treatment of an Ag surface with C_2H_4 (5%) + $^{16}O_2$ at P = 100 Pa and T = 470 K (1) followed by $^{18}O_2$ adsorption at $P = 10^{-2}$ Pa and T = 470 K (2). (ii) TPR spectra of CO_2 and C_2H_4O recorded after ethylene adsorption at the Ag surface containing both "nucleophilic" and "electrophilic" oxygen.[34] Reproduced with permission from ref 34. Copyright 1994 Elsevier.

Ag catalyst foil was heated to perform TPR spectroscopy. The resulting mass spectrometer signals (Figure 6ii) revealed that both ^{16}O (electrophilic) and ^{18}O (nucleophilic) are present in the CO_2 product (Figure 6ii, m/z 44 ($C^{16}O_2$) and m/z 48 ($C^{18}O_2$)), while only ^{16}O (electrophilic) is present in the EO product (Figure 6ii, m/z 29 ($CH^{16}O/C_2H_4{}^{16}O$) and m/z 31 ($CH^{18}O/C_2H_4{}^{18}O$)). The isotopic exchange of surface O* with the oxygen atoms in CO_2 probably also contributed to the final isotopic oxygen distribution of CO_2. These interesting results provide additional supporting evidence that electrophilic oxygen is responsible for the formation of EO and both nucleophilic oxygen and electrophilic oxygen are responsible for the formation of CO_2. In addition, the findings reveal that (i) ethylene oxide formation requires high pressures to sufficiently oxidize the Ag catalyst surface region that are difficult to access under UHV conditions and (ii) the active state of silver catalysts for ethylene epoxidation requires an oxidized surface region.

In situ Raman measurements of polycrystalline Ag surfaces under ethylene oxidation reaction conditions have been conducted by several research groups. Changes in the intensity of Raman peaks associated with oxygen species (630−640, 800−820, and 950−980 cm^{-1}) were commonly observed on different Ag catalysts during ethylene oxidation.[44,54,65−67] Boghosian et al. performed in situ Raman measurements on Ag films deposited on Y_2O_3-stabilized ZrO_2 (YSZ). The oxidized Ag gave rise to bands at 345, 815, and 870 (shoulder)

DOI: 10.1021/acscatal.9b03443
ACS Catal. 2019, 9, 10727−10750

cm^{-1} from oxygen species on Ag.[65] Although the Raman bands were not assigned, the intensity of all the bands was found to decrease during ethylene oxidation. Additional bands were observed at 1360 and 1590 cm^{-1} and were assigned to surface carbonaceous or adsorbed ethylene species.[65] Kondarides et al. compared the in situ Raman spectra of Ag/YSZ, Ag/quartz, and Ag/α-Al_2O_3 under ethylene oxidation.[67] For Ag/YSZ, bands were present at 240, 345, 815, 870, 980, and 1630 cm^{-1}, while only bands at 815 and 980 cm^{-1} were observed for Ag/quartz and Ag/α-Al_2O_3. The bands at 240 and 315 cm^{-1} may have come from the YSZ support. On Ag/YSZ, switching from $^{16}O_2$ to $^{18}O_2$ gave rise to an isotopic red shift of 20 cm^{-1} for the 815 cm^{-1} band, which suggested that these bands may arise from the O−O stretching vibration of molecularly adsorbed O_{2a} species. Upon introduction of C_2H_4 over the preoxidized Ag surface, the 980 cm^{-1} band grew in intensity and was proposed to be from surface carbonate species.[67] This assignment is not likely, since bulk $Ag_2(CO_3)$ vibrates at ∼1045 cm^{-1}. The 980 cm^{-1} band is more consistent with the O−O vibration of molecular O_2 species adsorbed on partially oxidized Ag.[68]

Millar et al. investigated polycrystalline Ag that was highly defective and detected Raman bands at 640, 780, and 960 cm^{-1} that were assigned to subsurface atomic O_{subs} species situated in the vicinity of surface dislocations, surface Ag═O sites formed on silver atoms modified by the presence of subsurface O_{subs} and molecularly adsorbed O_{2a}^- species stabilized on subsurface oxygen-modified surface silver sites, respectively.[54] During ethylene oxidation (1 bar and 473 K), the intensity of the bands at 640 and 780 cm^{-1} diminished with the preferential consumption of the 780 cm^{-1} band.[54]

A representative Raman spectrum under flowing O_2 at 201 °C (474 K) for Ag powder is shown in Figure 7a and exhibits two bands at 800 and 956 cm^{-1}.[66] The 800 and 956 cm^{-1} Raman bands both undergo isotopic shifts of 20−24 cm^{-1} to lower wavenumber upon exposure to $^{18}O_2$, indicating the ability of both of these surface ^{16}O containing species to readily exchange with gas-phase molecular $^{18}O_2$. These bands were assigned to Ag−O−Ag (800 cm^{-1}) and Ag═O species (956 cm^{-1}) species. The isotopic ratio of the shift for Ag═O is calculated as 1.0269, which deviates from 1.04−1.05 for M═O species.[69] Hence, the 956 cm^{-1} band should be assigned to other oxygen species. Exposure of the preoxidized Ag to flowing H_2O at low temperatures creates a new surface oxygen species at 866 cm^{-1} that almost vanishes upon heating to 201 °C (474 K). The 866 cm^{-1} band does not change position upon exposure to flowing D_2O, indicating that this new surface oxygen species does not contain any −OH/−OD bonds. Although CO_2 is known to complex with surface O* to form surface CO_3* intermediates,[37,70] surface carbonates were not detected when flowing CO_2/He was exposed to the preoxidized Ag powder. A possible explanation for the absence of surface carbonate species is that CO_2 does not readily adsorb on a fully oxidized Ag surface.[37]

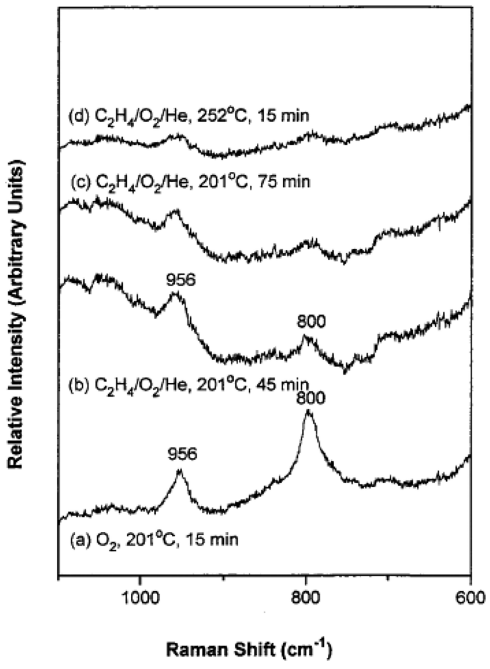

Figure 7. In situ Raman spectra of preoxidized polycrystalline silver powder obtained upon exposure to different reaction environments.[66] Reproduced with permission from ref 66. Copyright 1999 American Chemical Society.

Exposure of the silver powder catalyst to the reactive environments of C_2H_4/O_2/He, as well as C_2H_4/He, selectively consumes the oxygen species associated with the Raman band at 800 cm^{-1}. The intensity of the oxygen species associated with the Raman band at 956 cm^{-1} band only mildly decreases upon extended ethylene oxidation at 201 °C (474 K) and significantly decreases at 252 °C (525 K) during ethylene oxidation. The decrease in the intensity of the Raman band at 956 cm^{-1} at 252 °C (525 K) may arise from several scenarios: (i) consumption by the ethylene oxidation reaction, (ii) desorption of surface O*, or (iii) sintering of the Ag powder that would decrease the SERS effect. It is not possible at present to determine which of these mechanisms or if all the mechanisms contribute to the decrease of the Raman band at 956 cm^{-1} at 252 °C (474 K) during ethylene oxidation. Additionally, preoxidation with $^{18}O_2$ further demonstrated that the oxygen species associated with the 788 cm^{-1} Raman band was selectively consumed during the $C_2H_4/^{16}O_2$/He reaction environment. The in situ Raman spectra, however, do reveal that the oxygen species associated with the Raman band at ∼800 cm^{-1} are involved with the ethylene oxidation reaction and that it is always present during ethylene oxidation with a diminished intensity.

Although all the in situ Raman studies essentially detected the same oxygen species on Ag powders/films[54,66] and even single crystals[65] (∼630−650, 780−815, and 940−980 cm^{-1}), there is no agreement as to the assignments for the different oxygen species on Ag. The reason for this disagreement is that there were no supporting data for making any of the assignments and these studies predated the development of DFT computer codes. Applying recent DFT calculations to the Raman vibrations of oxygen species on Ag suggests that (i) the band at ∼960 cm^{-1} is associated with molecularly adsorbed O_{2a} on partially oxidized Ag, (ii) the band at ∼800 cm^{-1} arises from the interaction of surface atomic O_{surf} with subsurface atomic O_{sub} on partially oxidized Ag and hybrid O_{surf}═O_{sub} and (iii) bands below 700 cm^{-1} are associated with atomic O species on the surface and in the bulk lattice.[68] These preliminary calculations would suggest that the hybrid O_{surf}═O_{sub} species may be the active oxygen species present in Ag catalysts that are responsible for ethylene epoxidation.

Limited information is available in the literature about the steady-state reaction performance of unsupported Ag catalysts

DOI: 10.1021/acscatal.9b03443
ACS Catal. 2019, 9, 10727−10750

Table 1. Summary of Catalyst Compositions, Reaction Conditions, and Steady-State Catalytic Performance of Ag-based Catalysts for Ethylene Oxidation

	catalyst	feed conditions	temp (°C), pressure (bar)	ethylene conversion (%)	EO selectivity (%)	surface area (m^2/g)
1	unsupported Ag foil (electrorefined)[71]	23.8% C_2H_4, 7.19% O_2	237, 1	2.1	80	0.02
2	supported Ag nanowires, 175 nm, (Ag(100) surface dominant)/ α-Al_2O_3[15]	60% C_2H_4, 10% O_2	237, 1	~3	62	0.3
3	Ag (0.6 wt %, 200 nm)/ α-Al_2O_3[81]	2% C_2H_4, 7% O_2	237, 1		23	7
4	Ag (3.7 wt %, 400 nm)/ α-Al_2O_3[81]	2% C_2H_4, 7% O_2	237, 1		64	7
5	Ag (18.4 wt %, 400 nm)/SiO_2[81]	2% C_2H_4, 7% O_2	237, 1		43	200
6	Ag (11−13 wt %)/α-Al_2O_3[78]	10% C_2H_4, 10% O_2	267, 1.36	6.2	26	0.3
7	Ag (11−13 wt %)/α-Al_2O_3[11]	10% C_2H_4, 10% O_2, 1 ppm vinyl chloride	267, 1.36	1.5	47	0.3
8	Ag (11−13 wt %)/α-Al_2O_3[11]	10% C_2H_4, 60% O_2	267, 1.36		43	0.3
9	Ag (11−13 wt %)/α-Al_2O_3[11]	60%CH_4, 10% O_2	267, 1.36		42	0.3
10	Ag (11−13 wt %), Cs (68 ppm)/α-Al_2O_3 (coimpregnation)[11]	10% C_2H_4, 10% O_2,	267, 1.36	6.5	36	0.3
11	Ag (11−13 wt %), Cs (68 ppm)/α-Al_2O_3 (coimpregnation)[11]	10% C_2H_4, 60% O_2	267, 1.36		50	0.3
12	Ag (11−13 wt %), Cs (68 ppm)/α-Al_2O_3 (coimpregnation)[11]	60% C_2H_4, 10% O_2	267, 1.36		53	0.3
13	Ag (12 wt %)/α-Al_2O_3[9]	25% C_2H_4, 8% O_2, 2 ppm ethyl chloride	224, 17	10.5	75	0.6
14	Ag (12 wt %), Cs (350 ppm)/α-Al_2O_3[9]	25% C_2H_4, 8% O_2, 2 ppm ethyl chloride	224, 17	10.3	80	0.6
15	Ag (12 wt %), Cs (350 ppm), Re (200 ppm)/α-Al_2O_3[9]	25% C_2H_4, 8% O_2, 2 ppm ethyl chloride	224, 17	10.1	82	0.6
16	Ag (12 wt %), Cs (350 ppm), Re (200 ppm), Mo (150 ppm)/ α-Al_2O_3[9]	25% C_2H_4, 8% O_2, 2 ppm ethyl chloride	224, 17	9.8	83	0.6
17	Ag (15 wt %) + Cs + Re (Cs, 600 ppm, Re 400 ppm)/α-Al_2O_3 (coimpregnation)[79]	30% C_2H_4, 7.5% O_2, 1.85% CO_2, 0.1−0.5 ppm ethylene dichloride	226, 17	10.0	84	-
18	Re/Ag(15 wt %)-Cs/α-Al_2O_3 (Cs (600 ppm)-Re (400 ppm) sequential impregnation)[79]	30% C_2H_4, 7.5% O_2, 1.85% CO_2, 0.1−0.5 ppm ethylene dichloride	240, 17	7.1	64	-
19	Ag (35 wt %)/α-Al_2O_3 Cs (628 ppm), Li (33 ppm), Na (42 ppm), Re (440 ppm), $[SO_4]^{2-}$ (151 ppm), Mn (115 ppm)[72]	30% C_2H_4, 3% O_2, 0.4% C_2H_6, 1% CO_2, 6.3 ppm of C_2H_5Cl	240, 5.3	<1.5	87	1.3
20	Ag (11−13 wt %), Cu (0.5 mol %)/α-Al_2O_3[78] (alloy)	10% C_2H_4, 10% O_2	267, 1.36	12.2	36	0.3
21	Ag (13.18 wt %), Au (0.54 wt %)/α-Al_2O_3[82] (alloy)	6% C_2H_4, 6% O_2	255, 36	1.8	79	90

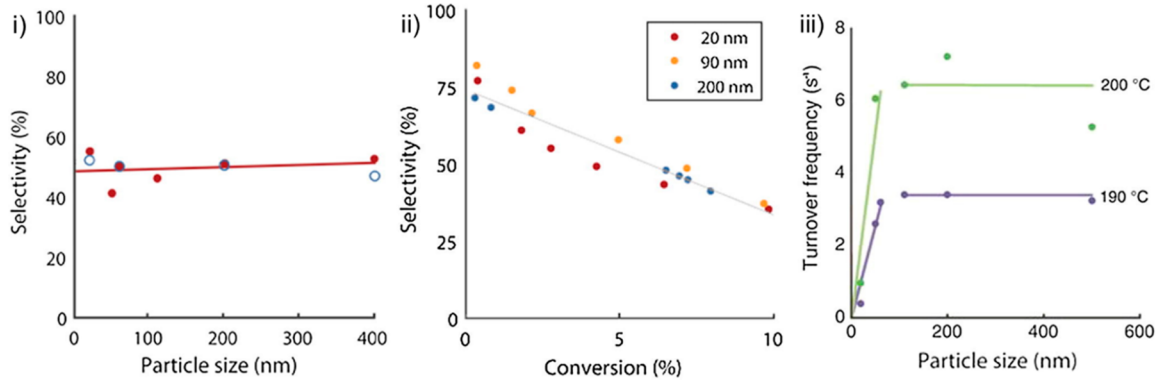

Figure 8. (i) Selectivity as a function of particle size for ethylene epoxidation of Ag/α-Al_2O_3 catalysts at constant conversion (2.8%). (ii) Selectivity versus conversion of silver catalyzed epoxidation. Catalysts with different particle size show that selectivity is conversion dependent, while all three (20, 90, and 200 nm Ag particles) catalysts follow the same trend line. (iii) Turnover frequency as a function of average Ag particle size for ethylene epoxidation of Ag/α-Al_2O_3 catalysts. Catalytic data obtained at atmospheric pressure with 8.5% O_2 and 30% ethylene flow in helium and a GHSV of 6000 h^{-1} at 190 and 200 °C and conversions ranging from 0 to 4.5%.[80] Reproduced with permission from ref 80. Copyright 2017 Elsevier.

for ethylene oxidation because the surface area of such catalysts is extremely low, which makes it somewhat challenging to detect ethylene oxidation products. For an electrorefined Ag foil (~0.02 m^2/g), an ethylene conversion of 2.1% and EO selectivity of 80% was obtained under reaction conditions of 257 °C (530 K) and 15 bar (see Table 1, entry 1).[71] This demonstrates that unsupported Ag catalysts can perform the ethylene epoxidation reaction and may serve as acceptable representative model catalysts.

2.3. Supported Ag Catalysts. *2.3.1. Protocols Employed in Studying Ethylene Oxidation by Supported Ag Catalysts.* The smaller metal particles present for oxide-supported Ag catalysts, most commonly on α-Al_2O_3 because of its support of choice for industrial applications, further increases the local surface area of the Ag particles (~1−5 m^2/g), but the surface Ag atoms only constitute a small fraction of the total Ag present in the particles.[9,72] With the exception of AES surface analysis that requires a conducting material not satisfied by the presence of the oxide support, the compatible characterization

DOI: 10.1021/acscatal.9b03443
ACS Catal. 2019, 9, 10727−10750

methods are the same as those indicated above for the Ag powders/films.

2.3.2. Surface Chemistry of Unpromoted Supported Ag Catalysts. The synthesis of supported Ag/α-Al_2O_3 catalysts is a crucial factor that determines the interactions between the Ag and the α-Al_2O_3 support. The α-Al_2O_3 support usually has a low surface area (~1 m^2/g) and porosity (<1 cm^3/g)[9,73] and may also have surface oxide impurities of S,[13,74,75] Si,[75] and Na.[75,76] Impurities such as surface oxides of S and Na are reported to be promoters for the ethylene epoxidation reaction by silver catalysts, with the influence of these surface impurities still not fully understood. The α-Al_2O_3 support is employed because its low surface area and basic nature minimizes further conversion of ethylene oxide to unselective reaction products (isomerization to CH_3CHO and combustion to CO_2).[77] In general, supported Ag/α-Al_2O_3 catalysts are prepared by impregnation of the α-Al_2O_3 support by aqueous silver nitrate[11,78] or silver oxalate solutions[9,79] with silver loadings of ~11−15 wt % typically reported as indicated in Table 1. The low surface area of the α-Al_2O_3 support and the high mobility of Ag are responsible for the large Ag particles with low dispersion on the α-Al_2O_3 support (see Table 1, entries 3−5). The average size of Ag nanoparticles on the low-surface-area α-Al_2O_3 support is sensitive to reducing/inert/oxidative environments. Exposing 15 wt % Ag/α-Al_2O_3 to $H_2/N_2/O_2$ treatments at 215 °C for 2 h results in average particle sizes of 28/62/76 nm, respectively, which indicates the important influence of environmental treatment on the Ag particle size.[80]

The size of the Ag particles on α-Al_2O_3 has been thought to influence the EO selectivity, with larger Ag particles yielding higher EO selectivity (23% on 200 nm Ag and 64% on 400 nm Ag, see Table 1, entries 3 and 4).[81] van den Reijen et al., however, recently demonstrated that this apparent trend is actually related to different conversions of ethylene, since EO selectivity decreases with ethylene conversion, and that at constant ethylene conversion the EO selectivity is constant for 20−400 nm Ag nanoparticles as shown in Figure 8i,ii.[80] There is, however, a strong relationship between Ag particle size and ethylene conversion, with the specific activity (TOF) linearly increasing from ~10−60 nm Ag particles and becoming independent of Ag particle size above 60 nm (Figure 8iii). The size distribution of the supported Ag particles investigated by van den Reijen, however, is still rather large (10−400 nm) since statistical analysis (Van Hardeveld−Hartog formalism) of different-sized fcc particles, such as Ag, indicates that the distributions of surface planes and defect sites are rather constant for particles larger than 6−8 nm.[83] Thus, to determine particle size effects, it would be necessary to investigate Ag particles <8 nm and especially particles <3 nm.

To better understand the performance of the Ag catalysts for ethylene oxidation reported in Table 1, the data in Table 1 have been plotted on van den Reijen et al.'s EO selectivity vs ethylene conversion curve in Figure 9. The exposed Ag planes or facets are also thought to influence the ethylene oxidation reaction. The results for the α-Al_2O_3-supported Ag nanowires, however, fall on van den Reijen et al.'s curve, indicating that the initially surface ordered nanowires and disordered Ag particles yield the same EO selectivity at the same ethylene conversion. This suggests that the initially ordered Ag nanowires underwent reconstruction during ethylene oxidation that made them indistinguishable from the conventional Ag/α-Al_2O_3 catalysts. The Ag−Au and Ag−Cu alloys appear to result in slightly higher EO selectivity values, since they fall just

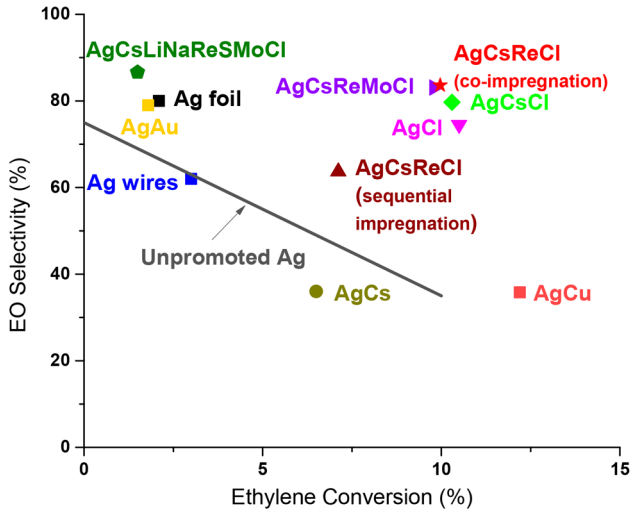

Figure 9. Selectivity versus conversion of ethylene over promoted and unpromoted Ag catalysts from published works in Table 1.

above the EO selectivity vs ethylene conversion curve. It has been proposed for ethylene oxidation by Ag catalysts that (i) defects on silver catalyze CO_2 production, but supporting evidence for this statement has not been provided,[53,84,85] and (ii) surface hydroxyl groups on high-surface-area alumina supports lead to significant ethylene adsorption and decrease in EO selectivity, but this is not supported by the high EO selectivity obtained with an Al_2O_3 support with 90 m^2/g at a relatively low ethylene conversion (Table 1, entry 23).[77,86]

2.3.3. Surface Chemistry of Promoted Ag Catalysts. As mentioned in the Introduction, promoters are introduced to the supported Ag/α-Al_2O_3 catalysts to enhance their selectivity to EO. The Cs, Re, and Mo promoters are introduced by impregnation of aqueous solutions of Cs_2CO_3,[9] or $CsNO_3$,[71] NH_4ReO_4,[9,71,79] or $HReO_4$,[87] and $(NH_4)_6Mo_7O_{24}{\cdot}4H_2O$,[9] respectively. The promoters can be introduced either with the Ag precursor or after the Ag impregnation step. The reported concentrations of the promoters vary from ~60 to 600 ppm as shown in Table 1. Although these values are quite small, it should be recalled that the surface area of the α-Al_2O_3 support is on the order of ~1 m^2/g and the surface area of the Ag nanoparticles is even lower, which makes the surface concentrations of the promoters a significant fraction of monolayer coverage.

The ethylene oxidation results for the promoted Ag catalysts are given in Table 1 and also plotted on the EO selectivity vs ethylene conversion curve in Figure 9. Jankowiak et al. reported the addition of only the Cs promoter to supported Ag/α-Al_2O_3 catalysts modestly increases the EO selectivity (Table 1, entries 6 and 10). However, in the absence of Cl and the other promoters, it has also been proposed that CsO_x complexes are formed and such complexes increase the oxygen adsorption energy and generate surface oxygen vacancies that in turn decrease the selectivity toward EO, but experimental supporting evidence was not provided.[9,59,88] The combination of Re + Cs has a positive effect on the EO selectivity. Impregnation of supported Ag/α-Al_2O_3 catalysts with oxides of Cs and Re further improved EO selectivity with optimum loadings of 350 ppm of Cs and 200 ppm of Re for the reported catalyst.[9] The sequence of impregnation for rhenium oxide on a supported Cs-Ag/α-Al_2O_3 catalyst was investigated by Ren et

DOI: 10.1021/acscatal.9b03443
ACS Catal. 2019, 9, 10727−10750

al.,[79] who found that the coimpregnated Ag-Cs-Re/α-Al_2O_3 catalyst results in superior catalytic performance relative to a sequentially impregnated Re/Ag-Cs/α-Al_2O_3 catalyst (Table 1, entries 17 and 18, and Figure 9). The improved performance of the coimpregnated catalyst may be related to the more intimate interaction of the promoters with Ag than with the alumina support.

The influence of Cs and Re promotion on the XPS Ag $3d_{5/2}$ spectra of oxidized supported Ag/α-Al_2O_3 catalysts is presented in Figure 10. The catalysts were given an oxidation

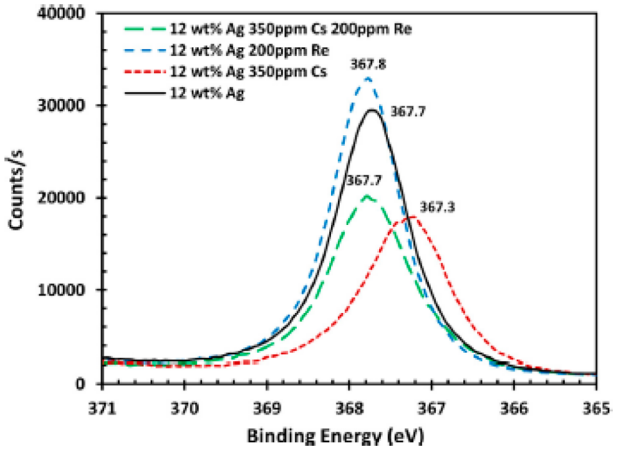

Figure 10. XPS Ag $3d_{5/2}$ spectra of oxidized 12 wt % Ag/α-Al_2O_3 catalyst (1) without promoter, (2) with 350 ppm of Cs, (3) with 200 ppm of Re, and (4) with 350 ppm of Cs and 200 ppm of Re after in situ pretreatment in 10% O_2/balance He at 280 °C for 12 h prior to directly transferring to UHV conditions for analysis. Only Ag $3d_{5/2}$ binding energy peaks are shown for clarity.[9] Reproduced with permission from ref 9. Copyright 2015 Elsevier.

treatment at 280 °C (553 K) and then directly transferred to the UHV analysis chamber without exposure to ambient conditions.[9] The unpromoted Ag/α-Al_2O_3 catalyst exhibits a Ag $3d_{5/2}$ binding energy (BE) of 367.7 eV that is minimally perturbed in the presence of the Re promoter (BE of 367.8 eV). Upon the addition of the Cs promoter, however, the Ag $3d_{5/2}$ BE shifts to 367.3 eV, reflecting an electronic interaction between the Cs promoter and the surface region of the Ag particle. In the presence of both Cs and Re promoters, however, the Ag $3d_{5/2}$ BE shifts back to that of the initial unpromoted catalyst (367.7 eV). Such a change in the Ag $3d_{5/2}$ BE from only Cs promotion to Cs + Re promotion suggests a strong interaction between these two promoters that minimizes their interactions with the Ag particle (e.g., possible formation of $CsReO_4$ complexes). These are interesting observations, but it needs to be kept in mind that the XPS measurements were performed under UHV conditions of preoxidized supported Ag/α-Al_2O_3 catalysts and not during ethylene oxidation conditions that can dramatically restructure the catalyst and its interactions with the promoters in the absence of a Cl source. Furthermore, to fully understand the fundamental behavior of the promoters on supported Ag/α-Al_2O_3 catalysts, their molecular structures must also be determined as a function of environmental conditions.[9,59,85,88]

In contrast to the introduction of the aqueous inorganic oxide promoters, Cl is introduced during ethylene oxidation in the reaction feed (1−3 ppm) as gaseous organic chlorides such as vinyl chloride[11,84] and ethyl chloride[9] in order to maintain a constant surface concentration of Cl, since Cl is also being stripped from the catalyst during the ethylene oxidation reaction. Promotion with Cl has a dramatic positive effect on the EO selectivity (Table 1, entries 13−19, and Figure 9) in both the absence and presence of the ReO_x and CsO_x promoters.

New highly informative insights about the role of Cl promotion come have from recent ex situ STEM images of a supported Ag/α-Al_2O_3 catalyst before and after the ethylene oxidation reaction, without and with vinyl chloride promotion, which are presented in Figure 11.[84] The initial Ag particle grows and forms open voids during ethylene oxidation in the absence of Cl promotion. The pores were reported to only increase the surface area of Ag by ∼2% while they decreased EO selectivity by ∼12% after 60 h of reaction. The formation of cavities in the Ag particle reflects that the entire silver particle may be participating in the ethylene epoxidation reaction with atomic oxygen migrating throughout the Ag particles. The stacking faults and eventually the nucleation of voids in the Ag particle may be a result of continuous transportation of atomic oxygen along the Ag particle grain boundaries. In the presence of the Cl promoter, which was

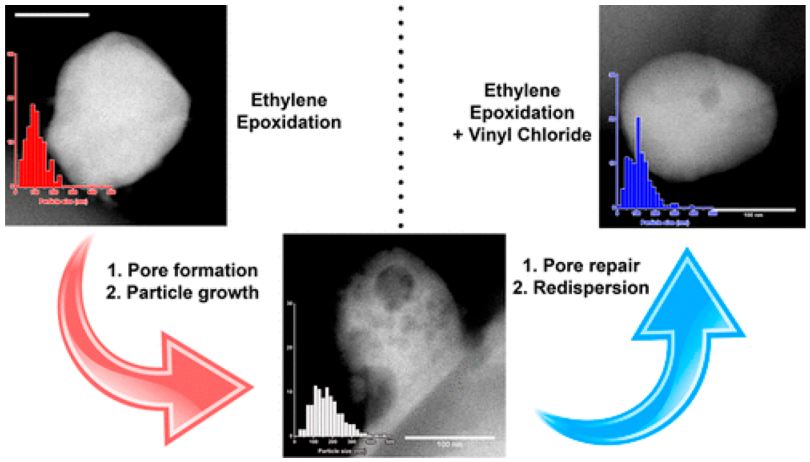

Figure 11. Ex situ STEM images under UHV showing restructuring of a supported Ag/α-Al_2O_3 catalyst before and after exposure to ethylene oxidation reaction conditions without and with vinyl chloride (VC) promotion. Catalyst test conditions: 20 bar, 225 °C, 5% C_2H_4, 10% O_2, (1 ppm VC), balanced by He.[84] Reproduced with permission from ref 84. Copyright 2018 American Chemical Society.

DOI: 10.1021/acscatal.9b03443
ACS Catal. 2019, 9, 10727−10750

Table 2. Summary of Proposed Effect of Promoters upon Ethylene Oxidation by Ag Catalysts

element	proposed promoting effect
Cl	(a) Geometrical effect: Cl and molecular O_2 competitively adsorb on reactive Ag sites, preventing O−O bond scission and increasing reactive surface dioxygen species (Ag(110) single crystal, O_2-TPD).[90] Cl blocks vacancies next to O_{surf}, preventing formation of C−Ag bonds required for the combustion pathway (Ag(111) single crystal, O_2-TPD;[47] Ag(110) single crystal, O_2-TPD;[91] supported catalyst, infrared spectra;[92] DFT[93,94]).
	(b) Electronic effect: Cl alters the transition state energies for conversion of OMC to EO vis-à-vis acetaldehyde (DFT).[85] Cl destabilizes O_{surf}, thereby making O_{surf} more electrophilic and enhancing interaction with ethylene C=C bonds (DFT).[95] Cl increases the concentration of surface electrophilic oxygen atoms (supported catalyst, in situ NAP-XPS).[53]
CsO_x	(a) Geometric effect: (i) Cs trapped at Ag step sites (supported catalyst, O_2-TPD;[89] supported catalyst, O_2-TPD + DRIFTS[96]).
	(b) Electronic effect: (i) Polarizable Cs^+ destabilizes surface intermediates or stabilizes transition states, perhaps by inducing an electric field (DFT).[97] (ii) "Dipole effect": increases the energy barrier for both ethylene oxide and acetaldehyde formation, but more significantly for acetaldehyde formation that creates a large separation in ΔE_A between the two products. Cs facilitates oxygen dissociation as the rate-determining step (DFT).[59,85]
ReO_x	(a) Geometric effect: ReO_x blocks steps and defect sites on Ag that shift oxygen adsorption and reaction to more uniform Ag terraces (supported catalyst, kinetics measurements).[98]
	(b) Electronic effect: $Re^{7+}O_x$ species shifts the Ag 3d binding energy to higher values, making the Ag site more electron-deficient, which increases the amount of electrophilic oxygen (supported catalyst, XPS).[9]
MoO_x	High-valent oxyanions may play a role similar to that of ReO_x (supported catalyst, speculation).[9]
SO_x	Geometric and electronic effect: Surface sulfate induces surface Ag reconstruction that surface enriches O_{elec}, facilitating selective transfer of an oxygen atom to ethylene (Ag(111) single crystal, XPS + DFT).[13]
CuO_x	Geometrical and electronic effect: under the reaction conditions, Cu tends to oxidize and form thin Cu oxide layers on top of the Ag particles, causing O_{sub} to migrate to the catalyst surface (DFT).[99,100] The O_{sub} weakens the bond strength of surface oxygen O_{surf}, thus facilitating the binding of the C=C double bond of ethylene to O_{surf}, forming EO (DFT).[99,101]
	Synergistic Effects between Promoters
CsO_x + ReO_x	The addition of Cs and Re to Ag catalyst reduces the potential energy between surface and subsurface oxygen, which promotes the transfer of oxygen between surface and subsurface (electrorefined Ag foil, O_2-TPD[71]).
	Highly polarizable Cs^+ transfers the e^- density to the e^--deficient $Ag^{\delta+}$ species. However, the interaction of the high-valent Re cation with $Ag^{\delta+}$ offsets the opposite effect of Cs^+, which minimizes their interactions with the Ag particle and potentially forms $CsReO_4$ complexes (supported catalyst, UHV-XPS[9]).
CsO_x + Cl	A combination of Cs and Cl added to Ag/α-Al_2O_3 lowers the O_2 desorption peak maximum temperature from 513 to 481 K (supported catalyst, O_2-TPD[89]).
	Synergistic interaction between Cs and Cl forms $CsCl_xO_y$ complexes and reduces oxygen surface vacancy formation (Ag(111) single crystal and supported catalyst, TPR;[43,51] DFT[88]).
ReO_x + Cl	Synergy between Re and Cl further reduces ethylene oxidation activity and increases EO selectivity (supported catalyst, steady-state reaction[9]).

cofed as vinyl chloride, the voids were repaired during ethylene oxidation with a corresponding increase in EO selectivity. This observation suggests that the Cl is acting as a structural promoter suppressing defective sites on the Ag particle that may be responsible for lower EO selectivity of unpromoted Ag/α-Al_2O_3 catalysts.[53,88] The results also demonstrate that silver particle size and morphology evolve dynamically and reversibly as a function of the reaction conditions. While sintering is evident during ethylene epoxidation, addition of chlorine results in smaller particles through a chlorine-induced redispersion mechanism. These insights add further support to the view that the active phase in heterogeneous catalysts is strongly dependent upon the reaction conditions.

Several studies have proposed that promoters enhance EO selectivity by formation of smooth and defect-free silver surfaces that has been ascribed to a "geometric effect". This hypothesis has only been shown for Cl promotion as shown in Figure 11 but still not demonstrated for the inorganic oxide promoters.[47,53,89]

Recently, Chen et al. performed kinetic measurements with an industrial EO catalyst containing six different promoters (Cs, Li, Na, Re, S, and Mn) as well as Cl and reported the highest selectivity of ∼87% among all catalysts summarized in Table 1, entry 19. Given that only one catalyst composition was investigated in this study, it is not possible to determine the contributions of the individual promoters and their possible synergistic interactions.

The catalytic data organized in Table 1 also provide much relevant information about the most effective reaction conditions for ethylene oxidation to EO by supported Ag/α-Al_2O_3 catalysts. The optimal reaction conditions for ethylene epoxidation are ∼230 °C and ∼10% ethylene conversion (Table 1, entries 13−17). The C_2H_4/O_2 ratio exerts a profound effect on the selectivity to ethylene oxide, with both C_2H_4-rich and O_2-rich feeds achieving higher selectivity over a stoichiometric feed of C_2H_4 and O_2 (Table 1, entries 6, 8, and 9 and entries 10−12)). The reaction pressure only plays a minor role in affecting EO selectivity, since reaction studies at both elevated and ambient pressures result in very similar EO selectivities (Table 1, entries 16 and 17).

2.4. Summary of Role of Promoters on Silver Catalysts. A summary of the reported proposals for the role of promoters upon ethylene oxidation by silver catalyst is organized in Table 2. The Cs and Cl promoters have been most extensively investigated, with the oxides of Re, Mo, and S promoters receiving only limited attention. The promoters have been categorized into geometric effects and/or electronic effects and are based on the assumption that a surface oxametallacycle (OMC) is a key surface reaction intermediate for ethylene oxidation.[30] Most of the proposed explanations in Table 2 have been reached from TPR measurements and spectroscopic observations and/or derived from DFT calculations. The content of Table 2 is divided into effects of single promoting elements and synergistic effects among Cs, Re, and Cl. It should be mentioned that current EO catalysts contain up to five to six metal salt promoters, in addition to Cl.[12,72] Thus, in any attempt to understand the role of one promoter, other promoters must be simultaneously incorporated into the discussion. The analysis of synergistic effects, however, is extremely scarce in the literature. Only a limited amount of works proposed promoting mechanisms of combined promoters of Cs + Re, Cs + Cl and Re + Cl using ex situ characterizations. In situ/operando investigations on the structure−activity relationship resulting from synergy between different promoters are much needed.

Although supported Ag/α-Al_2O_3 catalysts with good EO performance must have promoters, not much is known about the state of the promoters. The promoters may be (i)

DOI: 10.1021/acscatal.9b03443
ACS Catal. 2019, 9, 10727−10750

distributed on both the Ag nanoparticles and the α-Al_2O_3 support, (ii) distributed preferentially on either the Ag nanoparticles or the α-Al_2O_3 support, or (iii) combined as Cs−Re, Cs−Cl, or Re−Cl. Obtaining fundamental information about the states and distribution of the promoters would allow for better insights into how to modify the synthesis methods to produce better-performing EO catalysts. The absence of direct observations of the effect of promoters on Ag catalysts during ethylene oxidation makes it difficult to reach firm conclusions about the role of promoters. Hopefully, future in situ and operando spectroscopy investigations and DFT calculations will provide new fundamental insights about the role of promoters on Ag catalysts during the ethylene oxidation reaction.

3. KINETICS

The activation energy (E_a) and reaction order values for formation of both EO and CO_2 during ethylene oxidation conducted over a range of supported Ag catalysts and reaction conditions are presented in Table 3. The reported reaction order dependence on C_2H_4 partial pressure varies from −0.4 to 1 for EO and CO_2 formations. The reported reaction order dependence on O_2 partial pressure varies from ∼0.5 to 1 for EO formation and from ∼0.2 to 1 for CO_2 formation. The differences in the measured reaction orders can be ascribed to the variation in the types of catalysts and experimental conditions. Interestingly, many of the reported activation energies for formation of EO and CO_2 have similar values in each individual study[72,78,102,103] despite the larger differences among the different investigations. The most commonly reported activation energy was ∼90−100 kJ/mol. Reported activation energy values far from ∼90−100 kJ/mol, thus, are suspect. For example, a value of ∼25−50 kJ/mol suggests mass transfer limitations were probably present during these studies. The reported activation energy value of 212 kJ/mol is unusually large and was only obtained with a high dosing of Cl onto the surface of the Ag catalyst, indicating the inhibition of surface Cl on both ethylene epoxidation and combustion rates. Pre-exponential factors for the kinetic expressions were not reported by any of the studies.

Chen et al. tested an industrial EO catalyst supplied by Dow and examined the effect of cofeeding C_2H_5Cl in the reactant stream. It was found that C_2H_5Cl improves EO selectivity by simultaneously increasing the E_a values for both EO and CO_2 formation. Chen et al. also drew the following conclusions from their kinetic measurements: (i) dependence on gas-phase molecular O_2 partial pressure suggests that a species derived from molecular O_2 is involved in the kinetically relevant step, (ii) the same reaction orders on O_2 and C_2H_4 partial pressures and similar apparent activation energy values for EO and CO_2 formation suggest that a common reaction intermediate is involved in both reactions, and (iii) the introduction of Cl results in a decrease in surface coverage of oxygen-containing species, which is implied by a reaction order increase from 0.7 to 1 on the partial pressure of O_2 with increasing C_2H_5Cl concentration in the feed.[72]

Several kinetic models have been reported to account for the observed reaction rates for ethylene oxidation by supported Ag catalysts and are summarized in Table 4. The early kinetic studies reported by Harriott et al. for ethylene oxidation, with the absence and presence of the CO_2 and reaction products, proposed adsorbed molecular O_2 as the active oxygen species for both selective ethylene oxidation and total combus-

Table 3. Survey of Reaction Kinetics for Ethylene Oxidation by Supported Silver Catalysts

authors	catalyst	reaction conditions	E_a(EO) (kJ/mol)	$n(E_2)$	$n(O_2)$	$E_a(CO_2)$ (kJ/mol)	$n(E_2)$	$n(O_2)$
Kenson and Lapkin (1970)[104]	10 wt % Ag/Al_2O_3	3.44 bar, 55% C_2H_4, 45% air, 453−513 K	90	0	1	121	0	1
Force and Bell (1975)[102]	6.6 wt % Ag/Cab-O-Sil M5	0.055−0.182 bar C_2H_4, 0.156−0.390 bar O_2 443−493 K	∼24[a]	1	0.5	∼24[a]	1	0.5
Dettwiler et al. (1979)[103]	8 wt % Ag/pumice	0.002−0.03 bar C_2H_4, 0.05−0.2 bar O_2, 493−623 K	105	1	0.5	100	1	0.5
Jankowiak and Barteau (2005)[78]	Ag (11−13 wt %)/α-Al_2O_3	1.36 bar, 10−60% C_2H_4, 10−60% O_2, 500−540 K	54	0.19	0.65	54	−0.15	0.23
Jankowiak and Barteau (2005)[78]	Ag (11−13 wt %), Cu (0.5 mol %)/α-Al_2O_3	1.36 bar, 10−60% C_2H_4, 10−60% O_2, 500−540 K	49	0.2	0.48	58	−0.18	0.21
Chen et al. (2018)[72]	Ag (35 wt %)/α-Al_2O_3 Cs (628 ppm), Li (33 ppm), Na (42 ppm), Re (440 ppm), $[SO_4]^{2-}$ (151 ppm), Mn (115 ppm)	5.3 bar, 20−40% C_2H_4, 2−7% O_2, 0.4% C_2H_6, 1% CO_2, 1.5 ppm of C_2H_5Cl, 508−523 K	96	0.5	0.7	113	0.5	0.7
Chen et al. (2018)[72]	Same as above	5.3 bar, 20−40% C_2H_4, 2−7% O_2, 0.4% C_2H_6, 1% CO_2, 6.3 ppm of C_2H_5Cl, 508−523 K	212	−0.4	1	212	−0.4	1

[a]Determined from the reported data.

DOI: 10.1021/acscatal.9b03443
ACS Catal. 2019, 9, 10727−10750

Table 4. Survey of Reaction Rate Expressions of Ethylene Oxidation by Silver Catalysts[a]

authors (year), type of catalyst	kinetic expression
Klugherz and Harriot (1971), Ag (8.1 wt %)/α-Al_2O_3[105]	$r_1 = \frac{k_1 P_E P_0^2}{(1 + K_{E,1}P_E + K_{0,1}P_0 + K_{P,1}P_P)^2(1 + \sqrt{K_{S,1}P_0})^2}$
	$r_2 = \frac{k_2 P_E P_0^{1.5}}{(1 + K_{E,2}P_E + K_{0,2}P_0 + K_{P,2}P_P)^2(1 + \sqrt{K_{S,2}P_0})^2}$
Metcalf and Harriot (1972), Ag (8.1 wt %)/α-Al_2O_3[106]	$r_i = \frac{k_i P_E P_0^2}{(1 + K_1P_0^{0.5} + K_2P_0 + K_3P_E + K_4P_EP_0^{0.5} + K_5P_CP_0^{0.5} + K_6P_WP_0^{0.5})^2}$
Dettwiler et al. (1979), silver oxide[103]	$r_1 = k_1\frac{(C_2H_4)K_{C_2H_4}}{1 + (C_2H_4)K_{C_2H_4}}$
	$r_2 = k_2\frac{(C_2H_4)K_{C_2H_4}}{1 + (C_2H_4)K_{C_2H_4}}$
	$r_3 = k_3(C_2H_4O)$
Ghazali et al. (1983), Ag (11.3 wt %), Ba (1 wt %)/α-Al_2O_3;[117] Park & Gau (1987), Ag (25 wt %), Ba(2 wt %)/α-Al_2O_3[107]	$r_i = \frac{k_i k_E K_0 P_E P_0}{(1 + K_E P_E + K_0 P_0 + K_{E0}P_{P0})^2}$
Petrov et al. (1986), Ag (20 wt %), Ca/α-Al_2O_3[113]	$r_1 = \frac{k_1 P_E P_0}{1 + K_0P_0 + K_eP_E}$
	$r_2 = \frac{k_2 P_E P_0}{1 + K_0P_0 + K_eP_E}$
Stoukides and Paulou (1986), Ag film[118]	$r_1 = \frac{k_1K_EP_E - k_3K_{E0}P_{E0}^2}{1 + K_EP_E + K_{E0}P_{E0}^2}$
	$r_2 = \frac{k_2K_EP_E - k_3K_{E0}P_{E0}^2}{1 + K_EP_E + K_{E0}P_{E0}^2}$
Al-Saleh et al. (1987), Ag (7.96 wt %)/α-Al_2O_3[119]	$r_1 = \frac{k_1P_E^{0.6}P_0^{0.5}}{1 + K_{C,1}P_{CO_2}}$
	$r_2 = \frac{k_2P_E^{0.6}P_0^{0.5}}{1 + K_{C,2}P_{CO_2}}$
Borman and Westerterp (1995), Ag/α-Al_2O_3[115]	$r_i = \frac{k^iK_E^i\sqrt{K_0^i}P_E\sqrt{P_0}}{(1 + K_E^iP_E + \sqrt{K_0^iP_0} + K_C^iP_C + K_w^iP_W + K_{E0}^iP_{E0})^2}$
Lafarga et al. (2000) Ag (13.54 wt %), Cs (0.005%)/α-Al_2O_3[114]	$r_i = \frac{k_iP_EP_0^n}{(1 + K_e^iP_E)^2}$ $n = 0.5$ or 1
Carucci et al. (2010) Ag (15 wt %)/α-Al_2O_3 and polycrystalline silver plate[116]	model 1: $r_1 = \frac{k'P_E\sqrt{P_0}}{(1 + K_EP_E + \sqrt{K_0P_0})^2}$ [b]
	model 2: $r_1 = \frac{k'P_EP_0}{(1 + K_EP_E + \sqrt{K_0P_0})^2}$ [c]

[a]Definitions: r_1 = epoxidation reaction rate; r_2 = ethylene combustion reaction rate; r_3 = ethylene oxide combustion reaction rate; r_i = rate of ith reaction (i = 1−3, corresponds to r_1−r_3). [b]Assuming oxygen adsorption as rate-limiting step. [c]Assuming surface reaction as rate-limiting step.

tion.[105,106] Although adsorbed O_2* on Ag single crystals has been detected below room temperatures, the presence of surface dioxygen species on Ag single crystals, powders ,or supported catalysts above room temperature still has not been identified.[14,33,35,86,106−111] The nature of the molecular or atomic surface oxygen species on silver and its role in ethylene oxidation are still under debate. Both Langmuir−Hinshelwood (L-H) and Eley−Rideal (E-R, also recently referred to as Langmuir−Rideal[112]) reaction rate expressions, with different active species and rate-determining steps, have been proposed. Petrov et al. proposed a single site Eley−Rideal mechanism for ethylene conversion to EO and CO_2 that gives identical expressions for selective epoxidation and combustion.[113] More recently, it has generally been accepted that ethylene oxidation over Ag catalysts follows a single- or dual-site Langmuir−Hinshelwood mechanism with surface atomic oxygen as the active oxygen species for both selective epoxidation and total combustion.[107,114−116] In summary, ethylene oxidation reaction kinetic studies have not been able to distinguish between L-H or E-R (L-R) reaction mechanisms and the different types of oxygen species present on Ag during ethylene oxidation, reflecting the inability of just kinetic studies to establish the fundamental molecular events.

Although several studies contained promoted Ag catalysts,[107,113,114,117] rate expressions incorporating the effect of promoters have not been discussed or reported. In the future, comprehensive rate expressions should be developed to also

DOI: 10.1021/acscatal.9b03443
ACS Catal. 2019, 9, 10727−10750

account for the impact of the promoters on the kinetics of ethylene oxidation by Ag catalysts.

4. REACTION MECHANISM

4.1. Mechanistic Investigations with Ag Single-Crystal and Ag-Foil Catalysts. Given that the reaction between ethylene and adsorbed oxygen species on Ag single crystals has not been found to proceed under UHV conditions, Linic et al. examined the reverse reaction of ethylene oxide decomposition to ethylene and surface oxygen species by invoking the concept of "microscopic reversibility".[30] As already discussed above (section 2.1.2), from HREELS, DFT calculations, and TPR findings with the Ag(110) surface it was proposed that a surface oxametallacycle intermediate is formed at subambient temperatures and that it is the common reaction intermediate involved in formation of both EO and acetaldehyde, with the latter subsequently combusting to CO_2 and H_2O in the presence of oxygen. This ethylene oxidation reaction mechanism is now widely adopted, since it is the only reaction mechanism in the literature based on spectroscopy and DFT calculations.

Grant et al. were able to successfully investigate the ethylene oxidation reaction over Ag(111) with and without the presence of molecular weakly bound oxygen (proposed to be $O_{2,surf}$) by applying high pressures for adsorption of O_2 and C_2H_4. From angle-resolved (AR)-XPS and AES surface analysis, it was proposed that the oxygen species on Ag are present as molecular $O_{2,surf}$ and O_{surf} with the latter residing in the surface. The type of surface oxygen species on Ag(111) was controlled by selectively desorbing the weakly bound oxygen (proposed to be $O_{2,surf}$) from Ag(111) at 380 K, which allowed the preparation of Ag(111) surfaces with only the proposed O_{surf} or O_{surf} + $O_{2,surf}$ species. Both surfaces, however, were found to be able to produce EO (Figure 2). It was thus concluded that only the presence of the more strongly bound oxygen species (proposed to be O_{surf}) on Ag(111) is necessary and sufficient for production of ethylene oxide.[32] Additional characterization studies, however, are still required to confirm that the weakly adsorbed oxygen is indeed the proposed surface molecular $O_{2,surf}$ species. The observations by Grant et al. are in agreement with the findings of Bukhtiyarov et al. employing Ag foil and $^{18}O_2/^{16}O_2$ isotopes where weakly bound oxygen ($^{18}O_{x,surf}$, nucleophilic) does not yield $E^{18}O$ and only the presence of strongly bound oxygen ($^{16}O_{x,surf}$, electrophilic) forms $E^{16}O$.[53] Grant et al. identified acetaldehyde, acetic acid, and oxalic acid as reaction intermediates leading to CO_2 formation (note that these are gas-phase molecules and not surface reaction intermediates). Grant et al. also observed a kinetic isotope effect for CO_2 production when C_2D_4 was employed as the ethylene reactant, showing that C−D/C−H bond breaking and not C−C bond cleavage is involved in the rate-determining step for the combustion of both ethylene and EO. Although these studies have isolated the active surface oxygen species on Ag catalysts, whose molecular identity is still not completely established, they do not provide details about the reaction mechanism between adsorbed ethylene and surface oxygen species. On the basis of these observations, Grant et al. proposed the reaction mechanism of ethylene epoxidation that is different from the OMC mechanism. It was proposed that EO and CO_2 proceed via two distinctly different reaction pathways: EO proceeds via formation of an oxirane ring (cyclic C−O−C), and CO_2 proceeds via stripping of C−H bonds.[32]

4.2. Mechanistic Investigations with Supported Ag Catalysts. Transient analysis of products (TAP) is a powerful research tool in determining reaction mechanisms when it is combined with isotopic labeling. The TAP reactor system is a pulsed microreactor that allows controlling contact times between the reactant gases and the catalyst on the order of a few milliseconds and also provides variable time delays between pulses of reactants.[120] Gleaves et al. investigated ethylene oxidation by unpromoted supported Ag/α-Al_2O_3 with TAP studies.[120] In order to distinguish among the different active surface oxygen species on silver for ethylene oxidation, C_2D_4 was pulsed under anaerobic conditions on a catalyst that had been pretreated with 200 pulses of 100 L of O_2 at 274 °C.[108] It was assumed that if adsorbed molecular $O_{2,surf}$ was the active oxygen species on Ag, then the maximum EO yield would be expected to correspond to the highest concentration of $O_{2,surf}$ that would occur at time zero of the ethylene pulse. As demonstrated in Figure 12, the actual production of C_2D_4O, however, modestly peaked in the third pulse of C_2D_4, suggesting that atomic O_{surf} species were responsible for EO formation. Given that both O_{surf} and $O_{2,surf}$, the latter if present, would be at their maximum at the beginning of the ethylene pulse experiment, the assumption of this study is questionable. The continuing production of EO with number of pulses up to ∼30 s does support the above conclusion by Grant et al. and Bukhtiyarov et al. that the active surface oxygen species on Ag are the more strongly bound surface oxygen species that only form by high-temperature oxidation treatments. Only direct molecular spectroscopic monitoring of the nature of the surface oxygen species on silver would resolve which surface oxygen species are involved in the ethylene oxidation reaction pathways.[32]

5. DENSITY FUNCTIONAL THEORY (DFT) STUDIES

DFT is a relatively recent addition to the suite of tools used to study the ethylene oxidation reaction by Ag catalysts. The computational studies in this space can be categorized per the assumed nature of the surface under reaction conditions. A considerable body of research exists in exploring the properties of the metallic Ag system for ethylene oxidation, but a relatively smaller yet significant body of literature explores facets of bulk metal oxide (Ag_2O) and surface oxides. The electronic structure, chemistries, and energetics considerably vary depending on the surface, which are reviewed, compared, and contrasted in the works below.

5.1. Metallic Silver. The most commonly proposed mechanism for ethylene oxidation is the oxametallacycle (OMC) pathway,[30,121−123] as shown in Figure 13. Ethylene and adsorbed oxygen react to form a surface OMC intermediate either through a fully surface mediated Langmuir−Hinshelwood (L-H) mechanism (left) or via the Eley−Rideal (E-R) mechanism (right). Then formation of EO and acetaldehyde (AA) proceed via parallel isomerization steps of OMC with AA formed by the subsequent combustion steps yielding CO_2 and H_2O.

5.1.1. Oxametallacycle Intermediate. As shown in Figure 13, the surface oxametallacycle is a key intermediate in the proposed mechanism and has been identified on single-crystal surfaces using a combination of surface science and density functional theory (DFT) calculations, as discussed in detail earlier.[30,121,122] Two possible structures (OME and OMME) have been identified computationally,[30] which are distinguished by the number of metal atoms bonded to the surface

DOI: 10.1021/acscatal.9b03443
ACS Catal. 2019, 9, 10727−10750

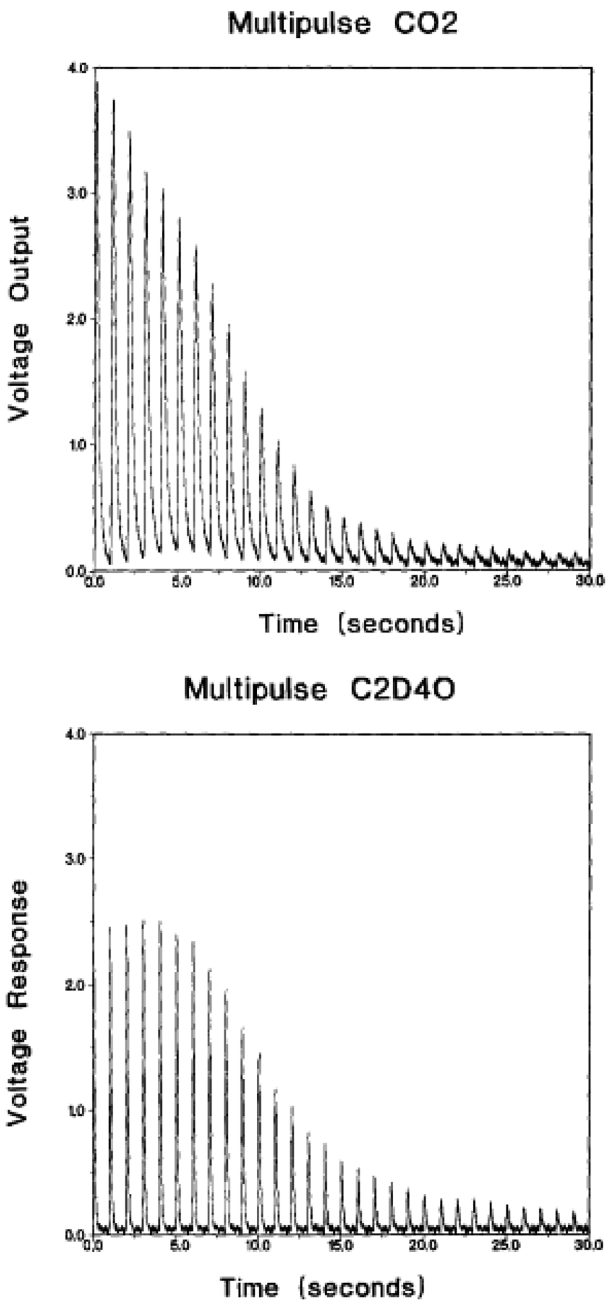

Figure 12. Amount of CO_2 (top) and C_2D_4O (below) formed as a function of pulses of anaerobic C_2D_4 (10^{17} molecules) at 547 K after pretreating the catalyst with 200 pulses of O_2 (10^{17} molecules) at 547 K.[108] Reproduced with permission from ref 108. Copyright 1990 Elsevier.

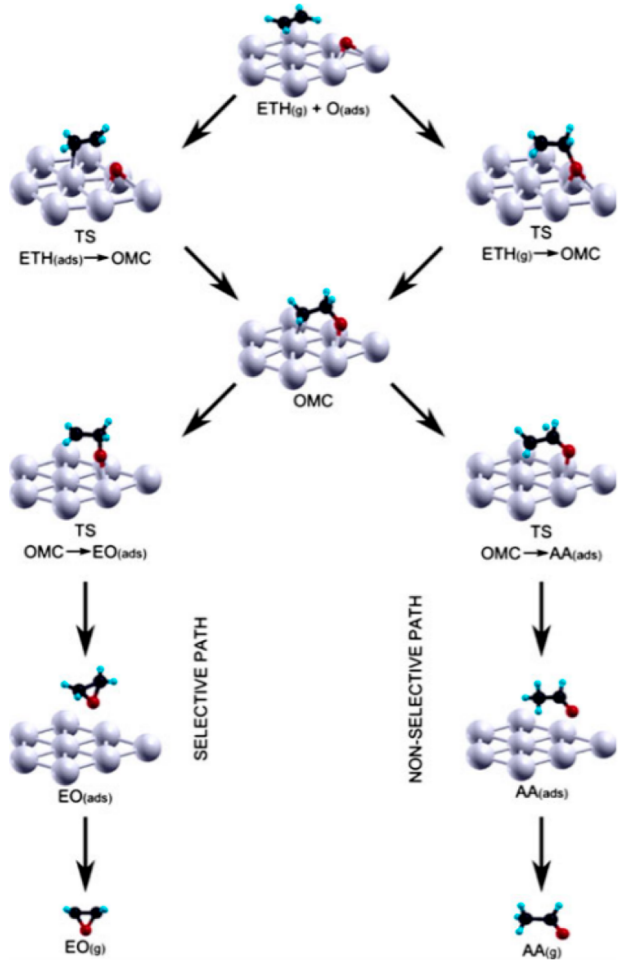

Figure 13. Mechanism of ethylene oxidation to EO and AA on Ag(111) along with the atomic structure of the intermediates and the transition state. (M, silver; O, red; C, black; H, cyan).[124] Reproduced with permission from ref 124. Copyright 2012 Springer Nature.

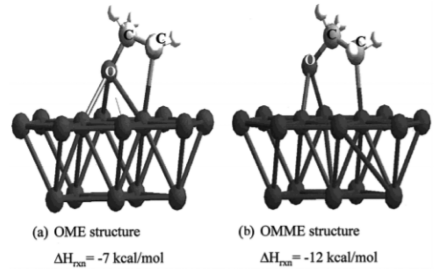

Figure 14. Proposed structures of the EO oxametallacycle: (a) OME structure; (b) OMME structure.[30] Reproduced with permission from ref 30. Copyright 2002 American Chemical Society.

OMC intermediate. As illustrated in Figure 14, the OME structure contains one silver atom bonded to the oxygen and a carbon of the backbone, while the OMME structure contains oxygen bonding to two silver atoms. Energetically, OME is slightly less stable than OMME due to the strain effect of the four-membered ring. While experimental evidence suggests that OME is the intermediate desorbing to form EO under TPD and UHV conditions,[30] the presence and the exact role of the surface OMC intermediate under relevant EO synthesis conditions has not been resolved.

5.1.2. Factors Controlling Selectivity. The mechanism shown in Figure 13 can explain the nearly 50% selectivity in the production of EO on unpromoted silver.[11] As noted earlier, the Barteau group suggested that the OMC intermediate was common to the production of both EO and acetaldehyde (AA), with AA being the precursor to the combustion products.[30,121,125] Figure 15 shows the first computational work to rationalize the selectivity of EO formation vis-a-vis the parallel combustion reaction pathway.[121] As depicted, the TS1 (to form EO) is primarily bound to the surface via its oxygen atom, while the TS2 binds with oxygen and carbon with a

DOI: 10.1021/acscatal.9b03443
ACS Catal. 2019, 9, 10727−10750

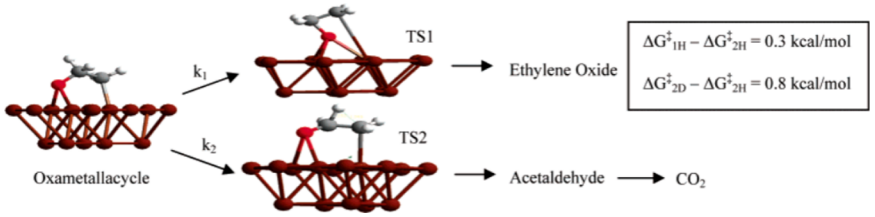

Figure 15. DFT-calculated structures of the competing reaction pathways for the conversion of the oxametallacycle intermediate. The inset shows the difference in Gibbs free energy of activation for the combustion versus selective pathway at T = 500 K and the difference for deuterated versus nonlabeled reactant at 0.1 monolayer and T = 420 K for the combustion pathways.[121] Reproduced with permission from ref 121. Copyright 2003 American Chemical Society.

structure similar to that of the OMC. The ratio of the reaction rates of these two reactions determines the selectivity; the rates themselves can be inferred from the computed free energies of the two transition states. Several computational studies have shown that the difference in the activation barrier for the two reactions (i.e., $E_a^{AA} - E_a^{EO}$) on unpromoted Ag(111) is small (4.8,[126] 1.9,[15] −5.8,[127] 5,[124] and −8.7[85] kJ/mol). After including the vibrational entropy and zero-point energy corrections, Linic and Barteau showed that the difference in the Gibbs free energy between the two transition states is 1.3 kJ/mol.[121] At 500 K, this represents a difference of less than 30% in the rates and a selectivity to EO of ∼50%; this is consistent with the observed value on unpromoted silver catalysts. Furthermore, DFT allows for calculating the expected kinetic isotope effect (see Figure 15). Since the formation of EO (TS1) does not involve C−H activation, its kinetic isotopic effect is expected to be less than that for the formation of AA (TS2). This agrees well with reported selectivity differences of C_2H_4 (49%) and C_2D_4 (73%).[109,121]

5.1.3. Promoter Effect. The promotion of EO synthesis by alkali metals has been explored using DFT. The dominant argument is that the alkali metals induce an electric field.[85,97] A Bader charge analysis shows that the OMC has a strong negative charge (−0.68e); the charge of the transition state to form EO (−0.34e) is higher than the transition state to form AA (−0.22e).[85] The argument is that, with a strong electric field induced by the alkali dopant, the charge transfer from OME to AA becomes more difficult in comparison to OME to EO, which means that the transition state of EO formation is stabilized in comparison to the transition state of AA formation. Computationally, the difference in the activation barrier of OMC to EO and AA is a metric for quantifying the selectivity (eq 6).[59,85]

$$\Delta E_a = E_A^{AA} - E_A^{EO} \quad (6)$$

Here, a higher value of ΔE_a indicates a higher selectivity. The selectivity gain of silver doped with different alkali is quantified by eq 7:[85]

$$\Delta\Delta E_a = \Delta E_a^{Ag+X} - \Delta E_a^{Ag} \quad (7)$$

Hus and Hellman showed that this selectivity gain correlated with the electronegativity, work function, and induced dipole moment of the dopant, implying the role of the electric field in altering the relative energies of the transition state.[85] Indeed, the behavior of the alkali metals can be mimicked by just introducing an electric field on an unpromoted Ag particle. Notably, the activation barriers for the two steps (i.e., AA and EO formation) increase on going from Li to Cs (relative to unpromoted Ag(111)) (Figure 16);[85] however, experimentally, the activity of EO synthesis increases with alkali doping. This

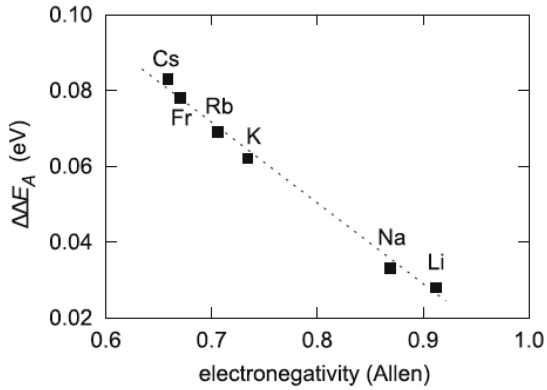

Figure 16. Gain in selectivity, measured as $\Delta\Delta E_a$ (as defined in eq 7), correlating with the electronegativity of the dopant atoms in the Allen scale.[85] Reproduced with permission from ref 85. Copyright 2018 Elsevier.

can be rationalized as follows. As shown in the kinetic modeling section, the dissociative adsorption of oxygen is a kinetically relevant step. Ren et al. have argued that the promotion effect of alkali on the overall activity is essentially due to the reduction in the activation barrier of dissociative adsorption of gaseous molecular O_2, which is consistent with O_2-TPD.[59,89,128] Consistent with this, DFT calculations by Hus and Hellman show that, in the presence of alkali metals on the surface, the activation barrier for molecular O_2 dissociation is lowered by 0.2−0.3 eV in comparison to pure Ag(111).[59] This reduction in the barrier can potentially outweigh the increase in the barriers of the subsequent steps.

Chlorine, another important promoter, tends to reduce the activity of Ag catalysts while substantially enhancing the EO selectivity, as has been observed experimentally. There has been some debate on the location of Cl on the Ag surface region. While experiments suggest Cl can diffuse into the subsurface,[52,129] multiple studies employing DFT-based phase diagrams have shown that the diffusion of Cl into the subsurface is energetically unfeasible at low coverages.[130,131] Torres et al. showed via DFT calculations that 0.25 ML of F, Cl, and Br on the surface lowered the energy of EO production by 0.5−1 eV and the AA production by ∼0.4−0.8 eV.[132] The authors further noted that the transition state for EO formation decreased by 0.35−0.5 eV and for AA formation decreased by 0.2−0.35 eV. These changes, in and of themselves, would imply that Br would have the greatest promotion activity followed by Cl. However, the authors argued that, in the presence of surface and subsurface Cl, there is (i) a relative lowering of the TS energy to form EO in comparison to AA of magnitude comparable to that seen for surface Cl alone and (ii) a decrease in the desorption barrier of EO by more than

DOI: 10.1021/acscatal.9b03443
ACS Catal. 2019, 9, 10727−10750

0.4 eV. Bromine, on the other hand, is too large to diffuse to a subsurface location. The combined effect of these factors results in Cl being the "best" halide promoter.

Hus and Hellman calculated that subsurface Cl increases $\Delta\Delta E_a$ by inducing an electric field effect similar to that of Cs, decreases the barrier for the formation of EO and AA, and increases the barrier for molecular O_2 dissociation. The net result is a decrease in activity while selectivity is enhanced. Combining Cs and Cl further modifies the electric field and affects selectivity and activity. Indeed, per their analysis, the trend in EO selectivity is Ag/Cs+Cl > Ag/Cl > Ag/Cs > Ag ,while the trend in rate was predicted to be Ag/Cs + Cl ≈ Ag > Ag/Cs > Ag/Cl.[85] Thus, there is a synergistic effect of increasing EO selectivity and maintaining activity upon codoping Cs and Cl.

5.1.4. Structure Sensitivity of a Catalytic Reaction. Nanoparticle catalysts expose different surface facets; in particular, nanoparticles of fcc metals such as Ag primarily expose (111) and (100) facets while steps and edges can expose facets such as (211) and (110). It is, therefore, important to understand the influence of the surface structure on the activity (structure sensitivity of a catalytic reaction). Engineering the surface composition and structure is one way to enhance the performance of a catalyst.[15] Previous discussions mainly focused on the Ag(111) surface since it is the most stable facet. Several studies have been conducted to understand the reactivity and EO selectivity on other more open facets.[15,126,127,133,134] These studies are also based on the OMC mechanism, and the metric for quantifying the selectivity is the energy difference in the transition state energies of isomerization of OMC to EO and AA.

The potential energy surfaces of ethylene epoxidation on different silver facets are compared in Figure 17. Clearly, the

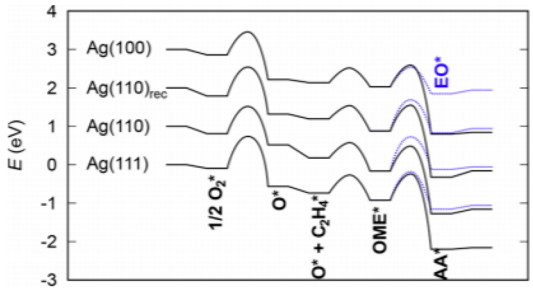

Figure 17. Reaction energy landscape for ethylene epoxidation on Ag(111), Ag(110), Ag(110)rec, and Ag(100). For clarity, the curves are staggered by 1 eV.[127] Reproduced with permission from ref 127. Copyright 2019 American Chemical Society.

relative energies of the transition states of the two isomerization reactions are facet dependent. In general, the trends across the closed and open facets identified by different groups are consistent, but differences also arise, perhaps due to the differences in the models, microkinetic formulations, or the chosen DFT codes and functionals. On the basis of eq 6, Linic and Barteau calculated that the EO selectivity of Ag(100) is greater than that of Ag(111), which is somewhat consistent with the experimental observations that supported Ag nanowires predominantly exposing Ag(100) are more selective than supported Ag particles exposing Ag(111) at very low ethylene conversions.[15] These experimental results, however, are suspect, since the Ag surface reconstructs during ethylene oxidation reaction conditions. Similarly, Zhu et al. found from DFT calculations that the trend in selectivity is Ag(110) > Ag(100) > Ag(111) > Ag(211). Interestingly, they found that the adsorption energy of OMC positively correlates with the EO selectivity on different silver facets. Using kinetic Monte Carlo (kMC) simulations, Huš and Hellman determined that EO selectivity follows Ag(100) > Ag(111) > $Ag(110)_{rec}$ > Ag(110) under the chosen conditions (1.34 bar, 400−625 K with 10% C_2H_4 and 10% O_2).[127]

The ethylene oxidation activity of the catalyst is another important aspect of this catalytic system. The kMC simulation comparing different silver facets found that for the overall turnover frequency (TOF) Ag(110) > Ag(100) > Ag(111). These studies clearly indicate the need for a detailed comparative analysis of the different facets of promoted Ag catalysts via microkinetic modeling based on ab initio energetics.

5.2. Silver Oxide. The silver catalyst is likely not purely metallic under the reaction conditions and possesses a thin silver oxide layer. Further, the selectivity of EO positively depends on the surface oxygen coverage that is not even addressed by the OMC pathway on a metallic Ag surface.[135] Mavrikakis and co-workers showed through DFT calculations that the subsurface oxygen can stabilize the surface adsorbates and transition states of many reactions on Ag(111), although they might inhibit EO synthesis.[136,137] van Santen and co-workers studied the mechanism of ethylene epoxidation on silver oxide surfaces, which essentially represents the limit of high surface and subsurface oxygen concentrations. Their DFT calculations (Figure 18) indicated that a direct oxidation of ethylene is likely possible in the absence of an oxygen vacancy, thereby circumventing the need for an surface OMC intermediate.[19,93,124,138,139] The bridging oxygen (Ag−O−Ag) was identified as an electrophilic oxygen that can attack the C═C bond to directly form EO. In the presence of an oxygen vacancy, however, the formation of OMC is more favorable, which would lead to total combustion since the activation barrier of AA formation is much smaller than that for EO. That is, an oxygen vacancy site on the Ag surface leads to unselective ethylene oxidation reactions. van Santen and co-workers further offered a consistent picture of the role of alkali and chloride promoters. Chloride poisons vacancies and prevents complete combustion. The Cs promoter, by itself, forms oxide clusters that destabilize the silver oxide surface and increase the formation of vacancies. The combination of Cs with chlorides forms cesium oxychlorides that stabilize the surface and reduce the surface vacancies, which would lead to increased EO selectivity.

Although it is argued that the bulk stable Ag oxides are not active under the reaction conditions, this body of literature offers important insights on its own right; specifically (i) it explains how an oxygen-rich surface could account for EO selectivity trends and (ii) it shows how the presence of electrophilic oxygen opens up new reaction pathways without the need for a surface OMC-type intermediate.

5.3. Reconstructed Silver. The computational studies on the metallic and bulk oxide systems bookend the surface oxygen coverage limits. There is increasing evidence, however, that under the reaction conditions the surface of Ag is oxidized and reconstructed. Ab initio phase diagrams, in this context, have been particularly insightful because they show what the surface structure should be under reaction conditions from a thermodynamic standpoint, assuming kinetic barriers can be overcome. A number of such analyses have been carried out,

DOI: 10.1021/acscatal.9b03443
ACS Catal. 2019, 9, 10727−10750

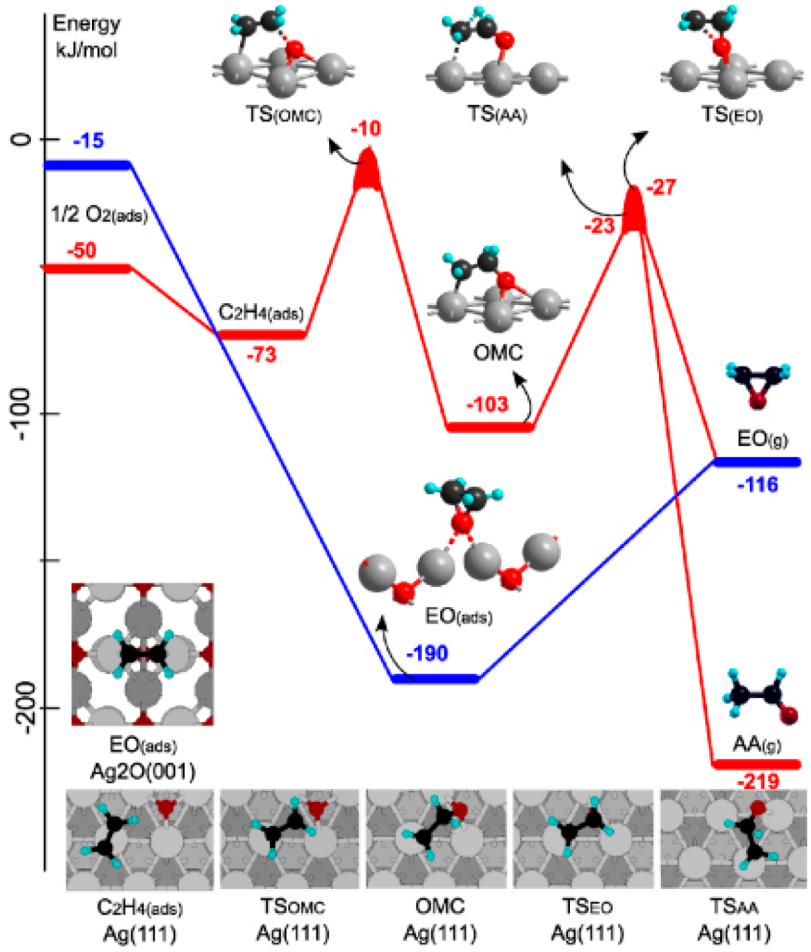

Figure 18. Reaction energy diagrams: the EO and AA formation paths through the OMC intermediate on Ag(111) surface (red lines (upper part)) and the direct EO formation path on $Ag_2O(001)$ surface (blue line (lower part)). The bottom figures represent the top views of the reaction intermediates. The energies are given with respect to surface + $1/2O_2(g)$ + $C_2H_4(g)$). Color code: Ag, gray; O, red (dark gray); C, black, H, cyan (light gray).[93] Reproduced with permission from ref 93. Copyright 2011 IOP Publishing.

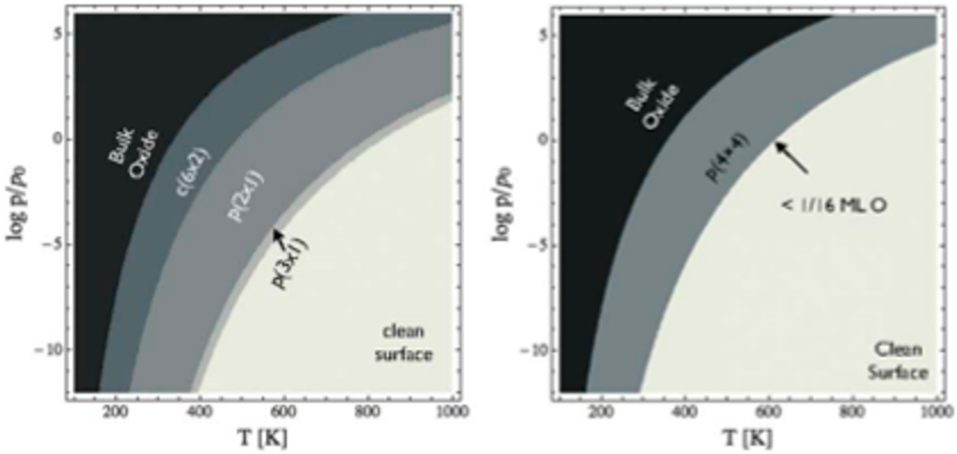

Figure 19. Ab initio phase diagram of the (left) Ag(110)−O system and (right) Ag(111)−O system calculated using bulk Ag and gaseous oxygen as reference states for Ag and O.[140] Reproduced with permission from ref 140. Copyright 2015 The Royal Society of Chemistry.

and Figure 19 shows the most recent phase diagram of the Ag(110) and Ag(111) facets.[140] These DFT calculations have suggested that the Ag(111) facet forms a p(4 × 4) reconstructed surface oxide, as shown in Figure 20, which is consistent with surfaces identified in scanning tunneling microscopy (STM) studies on Ag(111).[141−147] Other silver oxide surface reconstructions, such as the $c(3 \times 5\sqrt{3})$rect, and $p(4 \times 5\sqrt{3})$rect phases, have also been experimentally observed in STM studies. All three reconstructions are surface oxides of Ag_2O stoichiometry.

Few studies have explored the mechanism of EO formation on the reconstructed silver oxide surface. An early work

DOI: 10.1021/acscatal.9b03443
ACS Catal. 2019, 9, 10727−10750

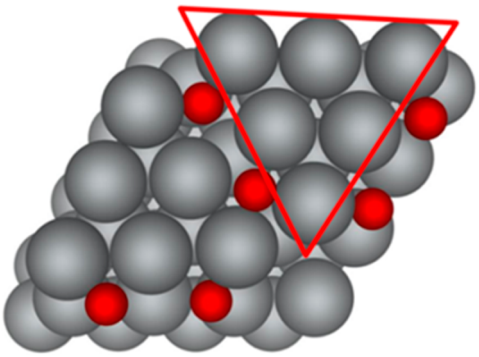

Figure 20. Top view of p(4 × 4) oxygen induced reconstructed Ag(111) with a surface stoichiometry of Ag_2O. Color code: Ag, silver; O, red. The silver atoms form Ag_6 triangles, and the oxygen atoms are located in the trough (furrow) between them.

suggested that the energetics of the OMC reaction pathway, wherein ethylene picks up a surface oxygen from the reconstructed surface, is more favorable than the Ag(111) + O system.[142] A subsequent study using an early interpretation of the structure of the surface oxide (an $Ag_{1.83}O$ surface which has been subsequently shown to be incorrect) showed that the conversion of OMC to acetaldehyde is energetically favored. More recently, DFT calculations on currently accepted structures of reconstructed Ag oxides showed that (i) the OMC pathway prefers the formation of acetaldehyde on the p(4 × 4)-O Ag(111) surface by 0.4 eV (Figure 21)[148] and (ii) the surface is rather mobile in that the Ag_6 triangles (Figure 20) can rotate about an axis perpendicular to the surface and this motion is key to favorable energetics on the reconstructed Ag(111) facet relative to the Ag(110) facet. The reconstructed surfaces, therefore, do not explain the observed selectivity. It is important to note that the direct epoxidation route, along the lines of that identified by van Santen and co-workers, has not been examined on reconstructed silver oxide surfaces.

5.4. Nature of the "Active" Oxygen Species. The electrophilic surface oxygen, which is argued to be particularly relevant for the ethylene epoxidation step, has been identified spectroscopically (corresponding to a core electron BE of 530 eV). The exact chemical identity of this species, however, has been rather elusive. Jones et al. analyzed a number of oxygenated silver surfaces (including the p(4 × 4) reconstructed surface) in terms of computed core electron BEs that can be compared with experimental XPS spectra.[149] It was shown that the O_{1s} BE of a variety of oxygen species on varied silver facets, including adsorbed atomic oxygen on an unreconstructed Ag surface, correlates linearly with their energy of adsorption. This correlation implies that a bound oxygen species with the necessary XPS signature for an electrophilic oxygen would have a large surface BE of >1.9 eV. Such oxygen atoms are then not covalently bonded to the surface (which would have rendered them electrophilic) and are instead ionically bonded and are, therefore, nucleophilic in nature. Consequently, they argued that none of the oxygen atoms on the reconstructed silver surfaces that they examined are electrophilic. Recently, it was shown that trace S impurities in ethylene can result in the formation of surface SO_x species on reconstructed $(7 \times \sqrt{3})$ and unreconstructed (111) silver surfaces. The surface SO_x species shows the characteristic XPS BE peak corresponding to an electrophilic oxygen that can easily insert an oxygen atom into ethylene to form EO relative

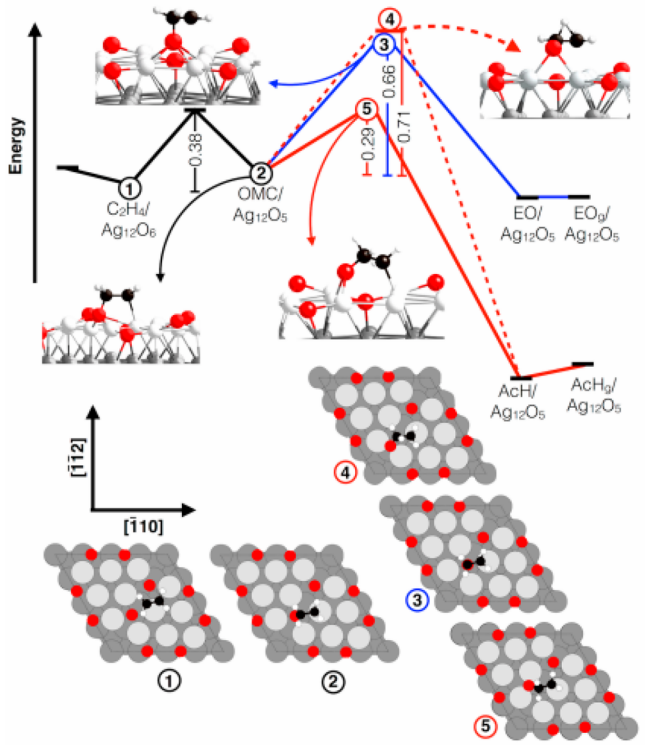

Figure 21. Minimum energy paths for AcH and EO formation on the p(4 × 4) oxygen induced reconstructed Ag(111) surface through the OMC mechanism. The oxygen atoms are colored red, the silver atoms in the Ag_6 triangles are light gray, the underlying silver is colored dark gray, carbon atoms are black, and oxygen atoms are white. State 1 shows the adsorbed ethylene, 2 the OMC, 3 the transition state to EO, 4 the transition state to AcH associated with the eclipsed hydrogen, and 5 the transition state to AcH associated with the staggered hydrogen. The activation energies for the elementary steps are given in eV.[148] Reproduced with permission from ref 148. Copyright 2016 American Chemical Society.

to the formation of acetaldehyde.[13,24] Another recent study proposed, through a combination of computed density of states and atomic charge analyses, that an O_3 species on Ag(111) would also be electrophilic.[150] It is unclear, though, that such highly reactive and unstable surface ozonide species form on industrial catalysts and, if they do, what their roles are in combination with other promoters.

6. MICROKINETIC MODELING

Microkinetic modeling is a computational technique that allows connecting atomic scale energetics to experimentally observable properties such as reaction rates, selectivity, etc. and inferring microscopic information about the reaction mechanism such as the surface coverage, flux carrying pathways, rate-determining steps, etc.[151,152] In contrast to kinetic expressions as discussed in section 4 which are derived from experimental data conducted over a narrow range of reaction conditions, microkinetic models are more general and can be applied to a broader range of reaction conditions.

To formulate a microkinetic model, one starts with a proposed active site and a detailed reaction mechanism comprising of possible elementary steps. The kinetic parameters of the elementary reactions (prefactor, activation barrier, sticking probability, etc.) can come either from surface science measurements or from ab initio calculations. Without

DOI: 10.1021/acscatal.9b03443
ACS Catal. 2019, 9, 10727−10750

Table 5. Summary of Reaction Network Suggested by Microkinetic Modeling[a]

	reaction	Stegelmann/Stoltze[155,157]	Huš/ Hellman[127,158]	Linic/Barteau[125]
	Adsorption/Desorption			
R1	$C_2H_4(g) + * \rightarrow C_2H_4*$	*	*	*
R2	$O_2(g) + 2* \rightarrow O_2**$	*	*	
R3	$O_2(g) + 2* \rightarrow 2O*$		*	*
R4	$O_2(g) + 2O* \rightarrow 2O/O*$		*	
R5	$C_2H_4(g) + O* \rightarrow CH_2CH_2O* + *$		*	
R6	$C_2H_4(g) + O* \rightarrow C_2H_4/O*$	*		
R7	$C_2H_4O(g) + O* \rightarrow C_2H_4O/O*$	*		
R8	$C_2H_4O* \rightarrow C_2H_4O(g) + *$		*	
R9	$CH_3CHO* \rightarrow CH_3CHO(g) + *$		*	
R10	$CO_2* \rightarrow CO_2(g) + *$	*		
R11	$H_2O* \rightarrow H_2O(g) + *$	*		
	Surface Reactions			
R12	$O_2** \rightarrow 2O*$	*	*	
R13	$C_2H_4* + O* \rightarrow CH_2CH_2O* + *$		*	*
R14	$C_2H_4/O* + O/O* \rightarrow CH_2CH_2O/O* + O*$	*		
R15	$CH_2CH_2O* \rightarrow C_2H_4O*$		*	*
R16	$CH_2CH_2O* \rightarrow CH_3CHO*$		*	
R17	$CH_2CH2O/O* \rightarrow C2H4O/O*$	*		
R18	$CH_2CH_2O/O* \rightarrow CH_3CHO/O*$	*		
	Combustion-Related Reactions			
R19	$CH_3CHO/O* + 6O* \rightarrow 2CO_2 + 4OH* + *$	*		
R20	$C_2H_4/O* + O* \rightarrow CH_2CHOH/O* + *$	*		
R21	$CH_2CHOH/O* + O* \rightarrow CH_2CHO/O* + OH*$	*		
R22	$CH_2CHO/O* + 5O* \rightarrow 2CO_2* + 3OH* + *$	*		
R23	$2OH* \rightarrow H_2O* + O*$	*		
	Diffusion			
R24	$O* + Ag_{subsurface} \rightarrow O{-}Ag_{subsurface} + *$	*		
R25	$O* + * \rightarrow * + O*$		*	

[a]An asterisk in columns 3−5 indicates if a particular step was included in a published model.

any prior assumptions of the important surface species or reactions (i.e., whether a particular reaction step is rate determining or if there is a most abundant surface intermediate), the equations of the model are numerically solved. The solution of the model is then used to determine important surface species, reaction pathways, etc. To write the equations of the model, one can adopt either of the two formalisms: the "mean-field" (MF) microkinetic model and kinetic Monte Carlo (kMC) simulations.[153,154] In MF models, the surface intermediates are presumed to be uniformly distributed on the surface. The formalism of MF models is a set of ordinary differential equations (ODEs) with the kinetics following the mass-action law and the surface state represented by an averaged surface coverage. MF fails when the diffusion of surface intermediates is slow and the adsorbate−adsorbate interaction is strong. To circumvent this, one can formulate kinetic Monte Carlo simulations, where the surface state is explicitly represented by the surface lattice or surface graph and solved by simulating the stochastic differential equations.

On the basis of the oxametallacycle (OMC) reaction mechanism, several microkinetic models have been proposed to account for the observed reaction kinetics for EO formation on unpromoted silver catalysts that incorporated the rate-limiting-step, selectivity-controlling step, most abundant surface intermediate, etc.[15,125−127,155,156] The elementary reaction steps of the reported microkinetic models from several leading research groups are summarized in Table 5.

Linic and Barteau proposed a simplified kinetic model involving a surface reaction between adsorbed C_2H_4 and O_{surf} proceeding through the oxametallacycle reaction intermediate without the formation of acetaldehyde (AA).[125] The kinetic parameters (prefactor and activation barrier) were extracted from first-principles calculations and temperature-programmed reaction (TPR) measurements. Stegelmann and Stoltze proposed a sophisticated and comprehensive reaction mechanism with two active sites, a metallic site (*) and a surface oxide site (O*).[155,156] For the modeling of transient kinetic experiments, the generation of subsurface oxygen was also included.[155] Similar to the case for Linic and Barteau, the microkinetic model was parametrized with rate constants estimated from DFT calculations and surface science measurements (vibrational frequency from spectroscopic measurements, activation energy and sticking probability from single-crystal kinetics). More recently, Huš and Hellman used kinetic Monte Carlo parametrization with DFT, explicitly including adsorbate−adsorbate interactions, and also examined the EO reaction on different silver facets (Ag(111), Ag(110), and Ag(100)).[127]

Although these microkinetic models included different elementary reaction steps and assumptions about the catalytic active sites, all of the models reached similar overall conclusions about the reaction mechanism. The selectivity-controlling reactions in the Stegelmann and Huš model are the isomerizations of OMC to EO and AA. All three models find that oxygen dissociation (oxide site formation) and the OMC formation step are kinetically relevant. Given that different catalytic active sites were invoked in the models, the predicted most abundant surface intermediate was not found to be the

DOI: 10.1021/acscatal.9b03443
ACS Catal. 2019, 9, 10727−10750

same in the models. The Stegelmann model considers surface oxide sites and predicts the surface is covered with electrophilic oxygen (O/O*) and ethylene is adsorbed on an oxide site (C_2H_4/O*), while the Huš model is based on a metallic surface for Ag(111) with low oxygen coverages. The Huš model agrees well with the kinetic experimental data on Ag(111) and slightly underpredicts the selectivity on Ag(110). The Stegelmann model is consistent with steady-state experimental data from different groups after adjusting the density of catalytic active sites ranging from single-crystal to supported Ag catalysts. Moreover, after the subsurface oxygen diffusion is included, the Stegelmann microkinetic model agrees well with TPR spectroscopy measurements. The selection of the common surface OMC reaction intermediate in these microkinetic studies probably contributed to the similar overall conclusions about the reaction mechanism. In summary, all microkinetic models adopt similar chemistries with some differences reflecting the assumptions of the active site; none of them consider alternative routes to EO formation such as the direct ethylene epoxidation route. Further, no microkinetic models have been formulated for the promoted Ag catalysts.

We end this section by briefly discussing the interrogative power of microkinetic models in the context of this reaction. As seen above, these models can offer mechanistic insights about ethylene oxidation; however, these models can also be used to address a number of "what if" questions that can potentially improve our understanding of this chemistry. These include questions such as the following. (i) What would the kinetics and thermochemistry have to be for a direct epoxidation route to be the dominant flux-carrying reaction? (ii) Does the model quantitatively capture experimental data and, if not, by how much should the energies obtained from DFT be changed to correctly match experiments, and if these changes are consistent with intrinsic errors of DFT,[159,160] (iii) is the role of the promoter purely geometric (i.e., they do not change the kinetics but they competitively adsorb and have a finite coverage on the surface), purely electronic (i.e., they have negligible surface coverage but substantially alter the kinetics), or both? (iv) What should the characteristics of the ideal promoter be (constrained by computational trends inferred from DFT such as that in Figure 16) to optimize selectivity and activity (in a manner similar to volcano plots in other heterogeneous catalytic chemistries)?

7. CONCLUSIONS AND PROSPECTS

This literature overview of ethylene oxidation by Ag catalysts provides many insights about the details of this complex catalytic system. The Ag surface must become oxidized to generate the catalytic active oxygen sites responsible for ethylene oxidation. There are multiple oxygen species on and in the silver surface, but their molecular structures are still not resolved. It appears that an electrophilic oxygen species, whose molecular structure is still to be determined, is responsible for ethylene epoxidation to EO. Promoters affect the number and distribution of the oxygen species on and in the silver surface and electronic charge of the surface and subsurface Ag atoms, but the molecular and electronic details are still not known. The ethylene oxidation reaction kinetics have been fit with both L-H and E-R rate expressions and the inability to distinguish between both rate expressions reflects the ambiguity of simplified kinetic expressions. Microkinetic models have been developed on metallic Ag surfaces on the basis of the proposed surface oxametallacycle intermediate reaction mechanism. Although several microkinetic models for the metallic Ag surface with different assumptions about the rate-determining step have been developed, all of the models fit the experimentally observed kinetics satisfactorily possibly because they are based on the common surface OMC intermediate. For silver oxide and reconstructed silver oxide surfaces, however, reaction pathways not involving the surface OMC intermediate have been developed from DFT calculations that depend on oxygen vacancies. The recent significant advances in DFT calculations and in situ/operando spectroscopic characterization during the ethylene oxidation reaction by Ag catalysts are poised to make great strides in advancing the fundamentals of the molecular/electronic structure−activity/selectivity relationships of this important oxidation reaction in the coming years.

AUTHOR INFORMATION

Corresponding Authors

*E-mail for S.R.: srr516@lehigh.edu.
*E-mail for I.E.W.: iew0@lehigh.edu.

ORCID

Tiancheng Pu: 0000-0002-4775-4294
Srinivas Rangarajan: 0000-0002-6777-9421
Israel E. Wachs: 0000-0001-5282-128X

Notes

The authors declare no competing financial interest.

ACKNOWLEDGMENTS

Financial support from NSF GOALI grant (# 1804104) is gratefully acknowledged.

REFERENCES

(1) Alper, J. *The Changing Landscape of Hydrocarbon Feedstocks for Chemical Production: Catalytic Conversion of Methane*; National Academy Press: 2016.
(2) Sattler, J. J. H. B.; Ruiz-Martinez, J.; Santillan-Jimenez, E.; Weckhuysen, B. M. Catalytic Dehydrogenation of Light Alkanes on Metals and Metal Oxides. *Chem. Rev.* **2014**, *114*, 10613−10653.
(3) United States Department of Energy. Ethane Storage and Distribution Hub in the United States; 2018.
(4) He, C.; You, F. Deciphering the True Life Cycle Environmental Impacts and Costs of the Mega-Scale Shale Gas-to-Olefins Projects in the United States. *Energy Environ. Sci.* **2016**, *9*, 820−840.
(5) Ren, T.; Patel, M.; Blok, K. Olefins from Conventional and Heavy Feedstocks: Energy Use in Steam Cracking and Alternative Processes. *Energy* **2006**, *31*, 425−451.
(6) Rebsdat, S.; Mayer, D. Ethylene Oxide. *Ullmann's Encycl. Ind. Chem.* **2001**, 1.
(7) Global and China Ethylene Oxide (EO) Industry Report, 2017−2021. *Res. China* **2017**, 137.
(8) Bukhtiyarov, V. I.; Knop-Gericke, A. Ethylene Epoxidation over Silver Catalysts. In*Nanostructured Catalysts: Selective Oxidations*; Knovel: 2011; pp 214−247.
(9) Diao, W.; Digiulio, C. D.; Schaal, M. T.; Ma, S.; Monnier, J. R. An Investigation on the Role of Re as a Promoter in Ag-Cs-Re/α-Al2O3 High-Selectivity, Ethylene Epoxidation Catalysts. *J. Catal.* **2015**, *322*, 14−23.
(10) Ayame, A.; Yoshida, T.; Yamaguchi, M.; Miura, H.; Sakai, Y.; Nojiri, N. Epoxidation of Ethylene over AgNaCl Catalysts. *J. Catal.* **1986**, *100*, 401−413.
(11) Jankowiak, J. T.; Barteau, M. A. Ethylene Epoxidation over Silver and Copper-Silver Bimetallic Catalysts: II. Cs and Cl Promotion. *J. Catal.* **2005**, *236*, 379−386.
(12) Matusz, M. United States Patent 5,739,075, 1998.

DOI: 10.1021/acscatal.9b03443
ACS Catal. 2019, 9, 10727−10750

(13) Jones, T. E.; Wyrwich, R.; Böcklein, S.; Carbonio, E. A.; Greiner, M. T.; Klyushin, A. Y.; Moritz, W.; Locatelli, A.; Menteş, T. O.; Niño, M. A.; Knop-Gericke, A.; Schlögl, R.; Günther, S.; Wintterlin, J.; Piccinin, S. The Selective Species in Ethylene Epoxidation on Silver. *ACS Catal.* **2018**, *8*, 3844−3852.
(14) van Santen, R. A.; de Groot, C. P. M. The Mechanism of Ethylene Epoxidation. *Adv. Catal.* **1987**, *35*, 265−321.
(15) Christopher, P.; Linic, S. Engineering Selectivity in Heterogeneous Catalysis: Ag Nanowires as Selective Ethylene Epoxidation Catalysts. *J. Am. Chem. Soc.* **2008**, *130*, 11264−11265.
(16) van Milligen, H.; VanderWilp, B.; Wells, G. J.; Outro; Outro; Outro. Enhancements in Ethylene Oxide/Ethylene Glycol Manufacturing Technology. *Shell Glob. Solut.* **2016**.
(17) Serafin, J. G.; Liu, A. C.; Seyedmonir, S. R. Surface Science and the Silver-Catalyzed Epoxidation of Ethylene: An Industrial Perspective. *J. Mol. Catal. A: Chem.* **1998**, *131*, 157−168.
(18) Montemore, M. M.; Van Spronsen, M. A.; Madix, R. J.; Friend, C. M. O2 Activation by Metal Surfaces: Implications for Bonding and Reactivity on Heterogeneous Catalysts. *Chem. Rev.* **2018**, *118*, 2816−2862.
(19) Özbek, M. O.; van Santen, R. A. The Mechanism of Ethylene Epoxidation Catalysis. *Catal. Lett.* **2013**, *143*, 131−141.
(20) Campbell, C. T. Atomic and Molecular Oxygen Adsorption on Ag(111). *Surf. Sci.* **1985**, *157*, 43−60.
(21) Grant, R. B.; Lambert, R. M. Basic Studies of the Oxygen Surface Chemistry of Silver: Chemisorbed Atomic and Molecular Species on Pure Ag(111). *Surf. Sci.* **1984**, *146*, 256−268.
(22) Bukhtiyarov, V. I.; Nizovskii, A. I.; Bluhm, H.; Hävecker, M.; Kleimenov, E.; Knop-Gericke, A.; Schlögl, R. Combined in Situ XPS and PTRMS Study of Ethylene Epoxidation over Silver. *J. Catal.* **2006**, *238*, 260−269.
(23) Carbonio, E. A.; Rocha, T. C. R.; Klyushin, A. Y.; Píš, I.; Magnano, E.; Nappini, S.; Piccinin, S.; Knop-Gericke, A.; Schlögl, R.; Jones, T. E. Are Multiple Oxygen Species Selective in Ethylene Epoxidation on Silver? *Chem. Sci.* **2018**, *9*, 990−998.
(24) Wyrwich, R.; Jones, T. E.; Günther, S.; Moritz, W.; Ehrensperger, M.; Böcklein, S.; Zeller, P.; Lünser, A.; Locatelli, A.; Menteş, T. O.; Niño, M. Á.; Knop-Gericke, A.; Schlögl, R.; Piccinin, S.; Wintterlin, J. LEED- i (V) Structure Analysis of the $(7 \times \sqrt{3})$Rect SO 4 Phase on Ag(111): Precursor to the Active Species of the Ag-Catalyzed Ethylene Epoxidation. *J. Phys. Chem. C* **2018**, *122*, 26998−27004.
(25) Datye, A. K. Electron Microscopy of Catalysts: Recent Achievements and Future Prospects. *J. Catal.* **2003**, *216*, 144−154.
(26) Zhou, W.; Wachs, I. E.; Kiely, C. J. Nanostructural and Chemical Characterization of Supported Metal Oxide Catalysts by Aberration Corrected Analytical Electron Microscopy. *Curr. Opin. Solid State Mater. Sci.* **2012**, *16*, 10−22.
(27) Rupprechter, G. Sum Frequency Generation and Polarization-Modulation Infrared Reflection Absorption Spectroscopy of Functioning Model Catalysts from Ultrahigh Vacuum to Ambient Pressure. *Adv. Catal.* **2007**, *51*, 133−263.
(28) Gao, F.; Wang, Y.; Goodman, D. W. Reaction Kinetics and Polarization-Modulation Infrared Reflection Absorption Spectroscopy (PM-IRAS) Investigation of CO Oxidation over Supported Pd-Au Alloy Catalysts. *J. Phys. Chem. C* **2010**, *114*, 4036−4043.
(29) Carter, E. A.; Goddard, W. A. The Surface Atomic Oxyradical Mechanism for Ag-Catalyzed Olefin Epoxidation. *J. Catal.* **1988**, *112*, 80−92.
(30) Linic, S.; Barteau, M. A. Formation of a Stable Surface Oxametallacycle That Produces Ethylene Oxide. *J. Am. Chem. Soc.* **2002**, *124*, 310−317.
(31) Tao, F. Design of an In-House Ambient Pressure AP-XPS Using a Bench-Top X-Ray Source and the Surface Chemistry of Ceria under Reaction Conditions. *Chem. Commun.* **2012**, *48*, 3812−3814.
(32) Grant, R. B.; Lambert, R. M. A Single Crystal Study of the Silver-Catalysed Selective Oxidation and Total Oxidation of Ethylene. *J. Catal.* **1985**, *92*, 364−375.
(33) Campbell, C. T.; Paffett, M. T. Model Studies of Ethylene Epoxidation Catalyzed by the Ag(110) Surface. *Surf. Sci.* **1984**, *139*, 396−416.
(34) Bukhtiyarov, V. I.; Prosvirin, I. P.; Kvon, R. I. Study of Reactivity of Oxygen States Adsorbed at a Silver Surface towards C2H4 by XPS, TPD and TPR. *Surf. Sci.* **1994**, *320*, L47−L50.
(35) Campbell, C. T. The Selective Epoxidation of Ethylene Catalyzed by Ag(111): A Comparison with Ag(110). *J. Catal.* **1985**, *94*, 436−444.
(36) Krüger, B.; Benndorf, G. Ethylene and Ethylene-Oxide Adsorption on Ag(110). *Surf. Sci.* **1986**, *178*, 704−715.
(37) Bowker, M.; Barteau, M. A.; Madix, R. J. Oxygen Induced Adsorption and Reaction of H2, H2O, CO and CO2 on Single Crystal Ag(110). *Surf. Sci.* **1980**, *92*, 528−548.
(38) Campbell, C. T.; Paffett, M. T. The Interactions of O2, CO and CO2 with Ag(110). *Surf. Sci.* **1984**, *143*, 517−535.
(39) Barteau, M. A.; Madix, R. J. Lateral Interaction Effects on the Reaction of CO2 and Oxygen Adsorbed on Ag(110). *J. Chem. Phys.* **1981**, *74*, 4144.
(40) Wachs, I. E.; Kelemen, S. R. The Interaction of Ethylene with Surface Carbonate and Hydroxide Intermediates on Silver. *J. Catal.* **1981**, *71*, 78−87.
(41) Zhu, M.; Wachs, I. E. Determining Number of Active Sites and TOF for the High-Temperature Water Gas Shift Reaction by Iron Oxide-Based Catalysts. *ACS Catal.* **2016**, *6*, 1764−1767.
(42) Barteau, M. A.; Madix, R. J. Low Pressure Oxidation of Ethylene on Ag(110): Possible Experimental Complications. *Surf. Sci.* **1981**, *103*, L171−L178.
(43) Grant, R. B.; Lambert, R. M. Ethylene Oxide Isomerisation on Single-Crystal Ag(111) in Atomically Clean and Cs-Moderated Conditions. *J. Catal.* **1985**, *93*, 92−99.
(44) Bao, X.; Pettinger, B.; Ertl, G.; Schlogl, R. In-Situ Raman Studies of Ethylene Oxidation at Ag(111) and Ag(110) under Catalytic Reaction Conditions. *Berichte der Bunsengesellschaft/Physical Chem. Chem. Phys.* **1993**, *97*, 322−325.
(45) Boudart, M.; Brenner, H. Principle of Microscopic Reversibility. In *Kinetics of Chemical Processes*; Wiley: 1991; pp 74−76.
(46) Grant, R. B.; Lambert, R. M. Alkali-Metal Promoters and Catalysis: A Single-Crystal Investigation of Ethylene Epoxidation on Cs-Doped Ag(111). *Langmuir* **1985**, *1*, 29−33.
(47) Campbell, C. T. Chlorine Promoters in Selective Ethylene Epoxidation over Ag(111): A Comparison with Ag(110). *J. Catal.* **1986**, *99*, 28−38.
(48) Campbell, C. T.; Paffett, M. T. The Role of Chlorine Promoters in Catalytic Ethylene Epoxidation over the Ag(110) Surface. *Appl. Surf. Sci.* **1984**, *19*, 28−42.
(49) Tan, S. A.; Grant, R. B.; Lambert, R. M. Secondary Chemistry in the Selective Oxidation of Ethylene: Effect of Cl and Cs Promoters on the Adsorption, Isomerisation, and Combustion of Ethylene Oxide on Ag(111). *J. Catal.* **1987**, *106*, 54−64.
(50) Campbell, C. T. Chlorine Promoters in Selective Ethylene Epoxidation over Ag(111): A Comparison with Ag(110). *J. Catal.* **1986**, *99*, 28−38.
(51) Grant, R. B.; Harbach, C. A. J.; Lambert, R. M.; Tan, S. A. Alkali Metal, Chlorine and Other Promoters in the Silver-Catalysed Selective Oxidation of Ethylene. *J. Chem. Soc., Faraday Trans. 1* **1987**, *83*, 2035−2046.
(52) Campbell, C. T.; Koel, B. E. Chlorine Promotion of Selective Ethylene Oxidation over Ag(110): Kinetics and Mechanism. *J. Catal.* **1985**, *92*, 272−283.
(53) Rocha, T. C. R.; Hävecker, M.; Knop-Gericke, A.; Schlögl, R. Promoters in Heterogeneous Catalysis: The Role of Cl on Ethylene Epoxidation over Ag. *J. Catal.* **2014**, *312*, 12−16.
(54) Millar, G. J.; Metson, J. B.; Bowmaker, G. A.; Cooney, R. P. In Situ Raman Studies of the Selective Oxidation of Methanol to Formaldehyde and Ethene to Ethylene Oxide on a Polycrystalline Silver Catalyst. *J. Chem. Soc., Faraday Trans.* **1995**, *91*, 4149−4159.
(55) Tang, Y.; Roberts, C. A.; Perkins, R. T.; Wachs, I. E. Revisiting Formic Acid Decomposition on Metallic Powder Catalysts: Exploding

DOI: 10.1021/acscatal.9b03443
ACS Catal. 2019, 9, 10727−10750

the HCOOH Decomposition Volcano Curve. *Surf. Sci.* **2016**, *650*, 103−110.
(56) Wood, B. J.; Wise, H. Surface Composition of PdAu and PdAg Catalysts by Auger Electron Spectroscopy. *Surf. Sci.* **1975**, *52*, 151−160.
(57) ter Veen, H. R. J.; Kim, T.; Wachs, I. E.; Brongersma, H. H. Applications of High Sensitivity-Low Energy Ion Scattering (HS-LEIS) in Heterogeneous Catalysis. *Catal. Today* **2009**, *140*, 197−201.
(58) Beitel, G.; Markert, K.; Wiechers, J.; Hrbek, J.; Behm, R. J. Characterization of Single-Crystal α-Al2O3 (0001) and (1120) Surfaces and Ag/Al2O3Model Catalysts by Atomic Force Microscopy. *Springer Ser. Surf. Sci.* **1993**, *33*, 71−82.
(59) Ren, D.; Xu, H.; Li, J.; Li, J.; Cheng, D. Origin of Enhanced Ethylene Oxide Selectivity by Cs-Promoted Silver Catalyst. *Mol. Catal.* **2017**, *441*, 92−99.
(60) Wachs, I. In Situ Raman Spectroscopy Studies of Catalysts. *Top. Catal.* **1999**, *8*, 57−63.
(61) Hartman, T.; Wondergem, C. S.; Kumar, N.; Van Den Berg, A.; Weckhuysen, B. M. Surface- and Tip-Enhanced Raman Spectroscopy in Catalysis. *J. Phys. Chem. Lett.* **2016**, *7*, 1570−1584.
(62) Schlücker, S. Surface-Enhanced Raman Spectroscopy: Concepts and Chemical Applications. *Angew. Chem., Int. Ed.* **2014**, *53*, 4756−4795.
(63) García-Vidal, F. J.; Pendry, J. B. Collective Theory for Surface Enhanced Raman Scattering. *Phys. Rev. Lett.* **1996**, *77*, 1163−1166.
(64) Lu, J.; Bravo-Suárez, J. J.; Takahashi, A.; Haruta, M.; Oyama, S. T. In Situ UV-Vis Studies of the Effect of Particle Size on the Epoxidation of Ethylene and Propylene on Supported Silver Catalysts with Molecular Oxygen. *J. Catal.* **2005**, *232*, 85−95.
(65) Boghosian, S.; Bebelis, S.; Vayenas, C. G.; Papatheodorou, G. N. In Situ High Temperature SERS Study of Ag Catalysts and Electrodes during Ethylene Epoxidation. *J. Catal.* **1989**, *117*, 561−565.
(66) Wang, C.-B.; Deo, G.; Wachs, I. E. Interaction of Polycrystalline Silver with Oxygen, Water, Carbon Dioxide, Ethylene, and Methanol: In Situ Raman and Catalytic Studies. *J. Phys. Chem. B* **1999**, *103*, 5645−5656.
(67) Kondarides, D. I.; Papatheodorou, G. N.; Vayenas, C. G.; Verykios, X. E. In Situ High Temperature SERS Study of Oxygen Adsorbed on Ag: Support and Electrochemical Promotion Effects. *Berichte der Bunsengesellschaft für Phys. Chemie* **1993**, *97*, 709−719.
(68) Liu, K.; Chen, T.; He, S.; Robbins, J. P.; Podkolzin, S. G.; Tian, F. Observation and Identification of an Atomic Oxygen Structure on Catalytic Gold Nanoparticles. *Angew. Chem.* **2017**, *129*, 13132−13137.
(69) Lee, E. L.; Wachs, I. E. In Situ Raman Spectroscopy of SiO2-Supported Transition Metal Oxide Catalysts: An Isotopic 18O-16O Exchange Study. *J. Phys. Chem. C* **2008**, *112*, 6487−6498.
(70) Backx, C.; De Groot, C. P. M.; Biloen, P.; Sachtler, W. M. H. Interaction of O2, CO2, CO, C2H4 and C2H4O with Ag(110). *Surf. Sci.* **1983**, *128*, 81−103.
(71) Jingfa, D.; Jun, Y.; Shi, Z.; Xiaohong, Y. Promoting Effects of Re and Cs on Silver Catalyst in Ethylene Epoxidation. *J. Catal.* **1992**, *138*, 395−399.
(72) Chen, C. J.; Harris, J. W.; Bhan, A. Kinetics of Ethylene Epoxidation on a Promoted Ag/α-Al2O3 Catalyst—The Effects of Product and Chloride Co-Feeds on Rates and Selectivity. *Chem. - Eur. J.* **2018**, *24*, 12405−12415.
(73) Shashkov, P.; Khomutov, G.; Yerokhin, A. UnIted States Patent 9,649,621 B2, 2012.
(74) Pansare, S. S.; Allison, J. D. An Investigation of the Effect of Ultra-Low Concentrations of Sulfur on a Co/γ-Al2O3 Fischer−Tropsch Synthesis Catalyst. *Appl. Catal., A* **2010**, *387*, 224−230.
(75) Van Der Laan, G. P.; Beenackers, A. A. C. M. Intrinsic Kinetics of the Gas-Solid Fischer−Tropsch and Water Gas Shift Reactions over a Precipitated Iron Catalyst. *Appl. Catal., A* **2000**, *193*, 39−53.
(76) Phung, T. K.; Herrera, C.; Larrubia, M. Á.; García-Diéguez, M.; Finocchio, E.; Alemany, L. J.; Busca, G. Surface and Catalytic Properties of Some γ-Al2O3 Powders. *Appl. Catal., A* **2014**, *483*, 41−51.
(77) Connor, P. T.; Kovenklioglu, S.; Shelly, D. C. Diffuse Reflectance Fourier-Transform IR Studies on the Role of Catalyst Support on Selectivity in Ethene Oxidation. *Appl. Catal.* **1991**, *71*, 247−263.
(78) Jankowiak, J. T.; Barteau, M. A. Ethylene Epoxidation over Silver and Copper-Silver Bimetallic Catalysts: I. Kinetics and Selectivity. *J. Catal.* **2005**, *236*, 366−378.
(79) Ren, D.; Cheng, G.; Li, J.; Li, J.; Dai, W.; Sun, X. X.; Cheng, D. Effect of Rhenium Loading Sequence on Selectivity of Ag−Cs Catalyst for Ethylene Epoxidation. *Catal. Lett.* **2017**, *147*, 2920−2928.
(80) van den Reijen, J. E.; Kanungo, S.; Welling, T. A. J.; Versluijs-Helder, M.; Nijhuis, T. A.; de Jong, K. P.; de Jongh, P. E. Preparation and Particle Size Effects of Ag/α-Al2O3 Catalysts for Ethylene Epoxidation. *J. Catal.* **2017**, *356*, 65−74.
(81) Goncharova, S. N.; Paukshtis, E. A.; Bal'zhinimaev, B. S. Size Effects in Ethylene Oxidation on Silver Catalysts. Influence of Support and Cs Promoter. *Appl. Catal., A* **1995**, *126*, 67−84.
(82) Rojluechai, S.; Chavadej, S.; Schwank, J. W.; Meeyoo, V. Catalytic Activity of Ethylene Oxidation over Au, Ag and Au-Ag Catalysts: Support Effect. *Catal. Commun.* **2007**, *8*, 57−64.
(83) Van Hardeveld, R.; Hartog, F. The Statistics of Surface Atoms and Surface Sites on Metal Crystals. *Surf. Sci.* **1969**, *15*, 189−230.
(84) Van Hoof, A. J. F.; Filot, I. A. W.; Friedrich, H.; Hensen, E. J. M. Reversible Restructuring of Silver Particles during Ethylene Epoxidation. *ACS Catal.* **2018**, *8*, 11794−11800.
(85) Huš, M.; Hellman, A. Dipole Effect on Ethylene Epoxidation: Influence of Alkali Metals and Chlorine. *J. Catal.* **2018**, *363*, 18−25.
(86) Yong, Y. S.; Kennedy, E. M.; Cant, N. W. Oxide Catalysed Reactions of Ethylene Oxide under Conditions Relevant to Ethylene Epoxidation over Supported Silver. *Appl. Catal.* **1991**, *76*, 31−48.
(87) Leszczynska-Sejda, K.; Benke, G.; Malarz, J.; Ciszewski, M.; Kopyto, D.; Piatek, J.; Drzazga, M.; Kowalik, P.; Zemlak, K.; Kula, B. Rhenium(VII) Compounds as Inorganic Precursors for the Synthesis of Organic Reaction Catalysts. *Molecules* **2019**, *24*, 1451.
(88) Özbek, M. O.; Önal, I.; van Santen, R. A. Chlorine and Caesium Promotion of Silver Ethylene Epoxidation Catalysts. *ChemCatChem* **2013**, *5*, 443−451.
(89) Atkins, M.; Couves, J.; Hague, M.; Sakakini, B. H.; Waugh, K. C. On the Role of Cs, Cl and Subsurface O in Promoting Selectivity in Ag/α-Al2O3 Catalysed Oxidation of Ethene to Ethene Epoxide. *J. Catal.* **2005**, *235*, 103−113.
(90) Kilty, P. A.; Sachtler, W. M. H. The Mechanism of the Selective Oxidation of Ethylene TO Ethylene Oxide. *Catal. Rev.: Sci. Eng.* **1974**, *10*, 1−16.
(91) Paffett, M. T.; Campbell, C. T. The Role of Chlorine Promoters in Catalytic Ethylene Epoxidation over the Ag(110) Surface. *Appl. Surf. Sci.* **1984**, *19*, 28−42.
(92) Force, E. L.; Bell, A. T. The Effect of Dichloroethane Moderation on the Adsorbed Species Present during the Oxidation of Ethylene over Silver. *J. Catal.* **1976**, *44*, 175−182.
(93) Ozbek, M. O.; Onal, I.; Van Santen, R. A. Ethylene Epoxidation Catalyzed by Chlorine-Promoted Silver Oxide. *J. Phys.: Condens. Matter* **2011**, *23*, 404202.
(94) Carter, E. A.; Goddard, W. A. Chemisorption of Oxygen, Chlorine, Hydrogen, Hydroxide, and Ethylene on Silver Clusters: A Model for the Olefin Epoxidation Reaction. *Surf. Sci.* **1989**, *209*, 243−289.
(95) Waugh, K. C.; Hague, M. The Detailed Kinetics and Mechanism of Ethylene Epoxidation on an Oxidised Ag/α-Al2O3 Catalyst. *Catal. Today* **2010**, *157*, 44−48.
(96) Amorim de Carvalho, M. C. N.; Passos, F. B.; Schmal, M. Study of the Active Phase of Silver Catalysts for Ethylene Epoxidation. *J. Catal.* **2007**, *248*, 124−129.
(97) Linic, S.; Barteau, M. A. On the Mechanism of Cs Promotion in Ethylene Epoxidation on Ag. *J. Am. Chem. Soc.* **2004**, *126*, 8086−8087.

DOI: 10.1021/acscatal.9b03443
ACS Catal. 2019, 9, 10727−10750

(98) Dellamorte, J. C.; Lauterbach, J.; Barteau, M. A. Rhenium Promotion of Ag and Cu-Ag Bimetallic Catalysts for Ethylene Epoxidation. *Catal. Today* **2007**, *120*, 182−185.
(99) Linic, S.; Jankowiak, J.; Barteau, M. A. Selectivity Driven Design of Bimetallic Ethylene Epoxidation Catalysts from First Principles. *J. Catal.* **2004**, *224*, 489−493.
(100) Nguyen, N. L.; De Gironcoli, S.; Piccinin, S. Ag-Cu Catalysts for Ethylene Epoxidation: Selectivity and Activity Descriptors. *J. Chem. Phys.* **2013**, *138*, 184707.
(101) Van den Hoek, P. J.; Baerends, E. J.; van Santen, R. A. Ethylene Epoxidation on Silver(110): The Role of Subsurface Oxygen. *J. Phys. Chem.* **1989**, *93*, 6469−6475.
(102) Force, E. L.; Bell, A. T. The Relationship of Adsorbed Species Observed by Infrared Spectroscopy to the Mechanism of Ethylene Oxidation over Silver. *J. Catal.* **1975**, *40*, 356−371.
(103) Dettwiler, H. R.; Baiker, A.; Richarz, W. Kinetics of Ethylene Oxidation on a Supported Silver Catalyst. *Helv. Chim. Acta* **1979**, *62*, 1689−1700.
(104) Kenson, R. E.; Lapkin, M. Kinetics and Mechanism of Ethylene Oxidation. Reactions of Ethylene and Ethylene Oxide on a Silver Catalyst. *J. Phys. Chem.* **1970**, *74*, 1493−1502.
(105) Klugherz, P. D.; Harriott, P. Kinetics of Ethylene Oxidation On. *AIChE J.* **1971**, *17*, 856−866.
(106) Metcalf, P. L.; Harriott, P. Kinetics of Silver-Catalyzed Ethylene Oxidation. *Ind. Eng. Chem. Process Des. Dev.* **1972**, *11*, 478−484.
(107) Park, D. Ethylene Epoxidation on a Silver Catalyst: Unsteady and Steady State Kinetics. *J. Catal.* **1987**, *105*, 81−94.
(108) Gleaves, J. T.; Sault, A. G.; Madix, R. J.; Ebner, J. R. Ethylene Oxidation on Silver Powder: A Tap Reactor Study. *J. Catal.* **1990**, *121*, 202−218.
(109) Cant, N. W.; Hall, W. K. Catalytic Oxidation. VI. Oxidation of Labeled Olefins over Silver. *J. Catal.* **1978**, *52*, 81−94.
(110) Ranney, J. T.; Gland, J. L.; Bare, S. R. The Desorption of Propylene Oxide from Oxygen Atom and Hydroxyl Covered Ag(110). *Surf. Sci.* **1998**, *401*, 1−11.
(111) Outka, D. A.; Madix, R. J.; Fisher, G. B.; DiMaggio, C. Oxidation of Sulfur Dioxide on Silver(110): Vibrational Study of the Structure of Intermediate Complexes Formed. *J. Phys. Chem.* **1986**, *90*, 4051−4057.
(112) Prins, R. Eley−Rideal, the Other Mechanism. *Top. Catal.* **2018**, *61*, 714−721.
(113) Petrov, L.; Eliyas, A.; Shopov, D. A Kinetic Model of Steady State Ethylene Epoxidation over a Supported Silver Catalyst. *Appl. Catal.* **1985**, *18*, 87−103.
(114) Lafarga, D.; Al-Juaied, M. A.; Bondy, C. M.; Varma, A. Ethylene Epoxidation on Ag-Cs/α-Al 2 O 3 Catalyst: Experimental Results and Strategy for Kinetic Parameter Determination. *Ind. Eng. Chem. Res.* **2000**, *39*, 2148−2156.
(115) Borman, P. C.; Westerterp, K. R. An Experimental Study of the Kinetics of the Selective Oxidation of Ethene over a Silver on α-Alumina Catalyst. *Ind. Eng. Chem. Res.* **1995**, *34*, 49−58.
(116) Carucci, J. R. H.; Halonen, V.; Eränen, K.; Wärnå, J.; Ojala, S.; Huuhtanen, M.; Keiski, R.; Salmi, T. Ethylene Oxide Formation in a Microreactor: From Qualitative Kinetics to Detailed Modeling. *Ind. Eng. Chem. Res.* **2010**, *49*, 10897−10907.
(117) Ghazali, S.; Park, D. W.; Gau, G. Kinetics of Ethylene Epoxidation on a Silver Catalyst. *Appl. Catal.* **1983**, *6*, 195−208.
(118) Stoukides, M.; Pavlou, S. Ethylene Oxidation on Silver Catalysts: Effect of Ethylene Oxide and of External Transfer Limitations. *Chem. Eng. Commun.* **1986**, *44*, 53−74.
(119) Al-Saleh, M. A.; Al-Ahmadi, M. S.; Shalabi, M. A. Kinetic Study of Ethylene Oxidation in a Berty Reactor. *Chem. Eng.* **1988**, *37*, 35−41.
(120) Morgan, K.; Maguire, N.; Fushimi, R.; Gleaves, J. T.; Goguet, A.; Harold, M. P.; Kondratenko, E. V.; Menon, U.; Schuurman, Y.; Yablonsky, G. S. Forty Years of Temporal Analysis of Products. *Catal. Sci. Technol.* **2017**, *7*, 2416−2439.
(121) Linic, S.; Barteau, M. A. Control of Ethylene Epoxidation Selectivity by Surface Oxametallacycles. *J. Am. Chem. Soc.* **2003**, *125*, 4034−4035.
(122) Jones, G. S.; Mavrikakis, M.; Barteau, M. A.; Vohs, J. M. First Synthesis, Experimental and Theoretical Vibrational Spectra of an Oxametallacycle on a Metal Surface. *J. Am. Chem. Soc.* **1998**, *120*, 3196−3204.
(123) Linic, S.; Piao, H.; Adib, K.; Barteau, M. A. Ethylene Epoxidation on Ag: Identification of the Crucial Surface Intermediate by Experimental and Theoretical Investigation of Its Electronic Structure. *Angew. Chem., Int. Ed.* **2004**, *43*, 2918−2921.
(124) Ozbek, M. O.; Onal, I.; Van Santen, R. A. Effect of Surface and Oxygen Coverage on Ethylene Epoxidation. *Top. Catal.* **2012**, *55*, 710−717.
(125) Linic, S.; Barteau, M. A. Construction of a Reaction Coordinate and a Microkinetic Model for Ethylene Epoxidation on Silver from DFT Calculations and Surface Science Experiments. *J. Catal.* **2003**, *214*, 200−212.
(126) Zhu, L.; Zhang, W.; Zhu, J.; Cheng, D. Mechanistic Insight into the Facet-Dependent Selectivity of Ethylene Epoxidation on Ag Nanocatalysts. *Appl. Catal., A* **2017**, *538*, 27−36.
(127) Huš, M.; Hellman, A. Ethylene Epoxidation on Ag(100), Ag(110), and Ag(111): A Joint Ab Initio and Kinetic Monte Carlo Study and Comparison with Experiments. *ACS Catal.* **2019**, *9*, 1183−1196.
(128) Jun, Y.; Jingfa, D.; Xiaohong, Y.; Shi, Z. Rhenium as a Promoter for Ethylene Epoxidation. *Appl. Catal., A* **1992**, *92*, 73−80.
(129) Bowker, M.; Waugh, K. C. The Adsorption of Chlorine and Chloridation of Ag(111). *Surf. Sci.* **1983**, *134*, 639−664.
(130) Roldán, A.; Torres, D.; Ricart, J. M.; Illas, F. The Chemistry of Chlorine on Ag(111) over the Sub-Monolayer Range: A Density Functional Theory Investigation. *Surf. Sci.* **2008**, *602*, 2639−2642.
(131) Gava, P.; Kokalj, A.; De Gironcoli, S.; Baroni, S. Adsorption of Chlorine on Ag(111): No Subsurface Cl at Low Coverage. *Phys. Rev. B: Condens. Matter Mater. Phys.* **2008**, *78*, 165419.
(132) Torres, D.; Illas, F.; Lambert, R. M. Towards an Understanding of Promoter Action in Heterogeneously Catalyzed Ethene Epoxidation: Why Chlorine Is the Best Halogen. *J. Catal.* **2008**, *260*, 380−383.
(133) Lukaski, A. C.; Barteau, M. A. Investigation of Ethylene Oxide on Clean and Oxygen-Covered Ag(110) Surfaces. *Catal. Lett.* **2009**, *128*, 9−17.
(134) Medlin, J. W.; Barteau, M. A. The Formation of Epoxides from Reactions of Oxametallacycles on Ag(110): A Density Functional Theory Study. *J. Phys. Chem. B* **2001**, *105*, 10054−10061.
(135) Christopher, P.; Linic, S. Shape- and Size-Specific Chemistry of Ag Nanostructures in Catalytic Ethylene Epoxidation. *ChemCatChem* **2010**, *2*, 78−83.
(136) Greeley, J.; Mavrikakis, M. On the Role of Subsurface Oxygen and Ethylenedioxy in Ethylene Epoxidation on Silver. *J. Phys. Chem. C* **2007**, *111*, 7992−7999.
(137) Xu, Y.; Greeley, J.; Mavrikakis, M. Effect of Subsurface Oxygen on the Reactivity of the Ag(111) Surface. *J. Am. Chem. Soc.* **2005**, *127*, 12823−12827.
(138) Ozbek, M. O.; Onal, I.; Van Santen, R. A. Why Silver Is the Unique Catalyst for Ethylene Epoxidation. *J. Catal.* **2011**, *284*, 230−235.
(139) Özbek, M. O.; Önal, I.; van Santen, R. A. Ethylene Epoxidation Catalyzed by Silver Oxide. *ChemCatChem* **2011**, *3*, 150−153.
(140) Jones, T. E.; Rocha, T. C. R.; Knop-Gericke, A.; Stampfl, C.; Schlögl, R.; Piccinin, S. Thermodynamic and Spectroscopic Properties of Oxygen on Silver under an Oxygen Atmosphere. *Phys. Chem. Chem. Phys.* **2015**, *17*, 9288−9312.
(141) Reichelt, R.; Günther, S.; Rößler, M.; Wintterlin, J.; Kubias, B.; Jakobi, B.; Schlögl, R. High-Pressure STM of the Interaction of Oxygen with Ag(111). *Phys. Chem. Chem. Phys.* **2007**, *9*, 3590−3599.

DOI: 10.1021/acscatal.9b03443
ACS Catal. 2019, 9, 10727−10750

(142) Bocquet, M. L.; Michaelides, A.; Loffreda, D.; Sautet, P.; Alavi, A.; King, D. A. New Insights into Ethene Epoxidation on Two Oxidized Ag(111) Surfaces. *J. Am. Chem. Soc.* **2003**, *125*, 5620−5621.
(143) Li, W. X.; Stampfl, C.; Scheffler, M. Insights into the Function of Silver as an Oxidation Catalyst by Ab Initio Atomistic Thermodynamics. *Phys. Rev. B: Condens. Matter Mater. Phys.* **2003**, *68*, 165412.
(144) Bocquet, M. L.; Sautet, P.; Cerda, J.; Carlisle, C. I.; Webb, M. J.; King, D. A. Specific Ethene Surface Activation on Silver Oxide Covered Ag(111) from the Interplay of STM Experiment and Theory. *J. Am. Chem. Soc.* **2003**, *125*, 3119−3125.
(145) Schmid, M.; Reicho, A.; Stierle, A.; Costina, I.; Klikovits, J.; Kostelnik, P.; Dubay, O.; Kresse, G.; Gustafson, J.; Lundgren, E.; Andersen, J. N.; Dosch, H.; Varga, P. Structure of Ag(111)-p(4 × 4)-O: No Silver Oxide. *Phys. Rev. Lett.* **2006**, *96*, 146102.
(146) Schnadt, J.; Michaelides, A.; Knudsen, J.; Vang, R. T.; Reuter, K.; Lægsgaard, E.; Scheffler, M.; Besenbacher, F. Revisiting the Structure of the p(4 × 4) Surface Oxide on Ag(111). *Phys. Rev. Lett.* **2006**, *96*, 146101.
(147) Schnadt, J.; Knudsen, J.; Hu, X. L.; Michaelides, A.; Vang, R. T.; Reuter, K.; Li, Z.; Lægsgaard, E.; Scheffler, M.; Besenbacher, F. Experimental and Theoretical Study of Oxygen Adsorption Structures on Ag(111). *Phys. Rev. B: Condens. Matter Mater. Phys.* **2009**, *80*, No. 075424.
(148) Jones, T. E.; Wyrwich, R.; Bocklein, S.; Rocha, T. C. R.; Carbonio, E. A.; Knop-Gericke, A.; Schlogl, R.; Gunther, S.; Wintterlin, J.; Piccinin, S. Oxidation of Ethylene on Oxygen Reconstructed Silver Surfaces. *J. Phys. Chem. C* **2016**, *120*, 28630−28638.
(149) Jones, T. E.; Rocha, T. C. R.; Knop-Gericke, A.; Stampfl, C.; Schlögl, R.; Piccinin, S. Insights into the Electronic Structure of the Oxygen Species Active in Alkene Epoxidation on Silver. *ACS Catal.* **2015**, *5*, 5846−5850.
(150) Kenge, N.; Pitale, S.; Joshi, K. The Nature of Electrophilic Oxygen: Insights from Periodic Density Functional Theory Investigations. *Surf. Sci.* **2019**, *679*, 188−195.
(151) Grabow, L. C.; Mavrikakis, M. Mechanism of Methanol Synthesis on Cu through CO2 and CO Hydrogenation. *ACS Catal.* **2011**, *1*, 365−384.
(152) Gokhale, A. A.; Kandoi, S.; Greeley, J. P.; Mavrikakis, M.; Dumesic, J. A. Molecular-Level Descriptions of Surface Chemistry in Kinetic Models Using Density Functional Theory. *Chem. Eng. Sci.* **2004**, *59*, 4679−4691.
(153) Reuter, K. First-Principles Kinetic Monte Carlo Simulations for Heterogeneous Catalysis: Concepts, Status, and Frontiers. In *Modeling and Simulation of Heterogeneous Catalytic Reactions*; Wiley: 2011; pp 71−111.
(154) Stamatakis, M.; Vlachos, D. G. Unraveling the Complexity of Catalytic Reactions via Kinetic Monte Carlo Simulation: Current Status and Frontiers. *ACS Catal.* **2012**, *2*, 2648−2663.
(155) Stegelmann, C.; Stoltze, P. Microkinetic Analysis of Transient Ethylene Oxidation Experiments on Silver. *J. Catal.* **2004**, *226*, 129−137.
(156) Stegelmann, C.; Schiødt, N. C.; Campbell, C. T.; Stoltze, P. Microkinetic Modeling of Ethylene Oxidation over Silver. *J. Catal.* **2004**, *221*, 630−649.
(157) Stoltze, P. Microkinetic Simulation of Catalytic Reactions. *Prog. Surf. Sci.* **2000**, *65*, 65−150.
(158) Huš, M.; Grilc, M.; Pavlišič, A.; Likozar, B.; Hellman, A. Multiscale Modelling from Quantum Level to Reactor Scale: An Example of Ethylene Epoxidation on Silver Catalysts. *Catal. Today* **2019**, *338*, 128−140.
(159) Rangarajan, S.; Maravelias, C. T.; Mavrikakis, M. Sequential-Optimization-Based Framework for Robust Modeling and Design of Heterogeneous Catalytic Systems. *J. Phys. Chem. C* **2017**, *121*, 25847−25863.
(160) Matera, S.; Schneider, W. F.; Heyden, A.; Savara, A. Progress in Accurate Chemical Kinetic Modeling, Simulations, and Parameter Estimation for Heterogeneous Catalysis. *ACS Catal.* **2019**, *9*, 6624−6647.

DOI: 10.1021/acscatal.9b03443
ACS Catal. 2019, 9, 10727−10750